Published in final edited form as:
Sci Transl Med. 2023 May 17; 15(696): eadg0675. doi:10.1126/scitranslmed.adg0675.

Clonally-Expanded, Thyrotoxic Effector CD8+ T cells Driven by *IL-21* Contribute to Checkpoint Inhibitor Thyroiditis

Melissa G. Lechner[1,*], **Zikang Zhou**[2], **Aline T. Hoang**[2,3,†], **Nicole Huang**[2,†], **Jessica Ortega**[2,†], **Lauren N. Scott**[2,†], **Ho-Chung Chen**[2], **Anushi Y. Patel**[2], **Rana Yakhshi-Tafti**[2,4], **Kristy Kim**[5], **Willy Hugo**[6], **Pouyan Famini**[1], **Alexandra Drakaki**[7], **Antoni Ribas**[7], **Trevor E. Angell**[8], **Maureen A. Su**[2,9]

[1]Division of Endocrinology, Diabetes, and Metabolism, UCLA David Geffen School of Medicine; Los Angeles, CA 90095.

[2]Department of Microbiology, Immunology, and Molecular Genetics, UCLA David Geffen School of Medicine; Los Angeles, CA 90095.

[3]Drexel Medical School; Philadelphia, PA 19129.

[4]Rosalind Franklin Medical School; Chicago, IL 60064.

[5]UCLA David Geffen School of Medicine; Los Angeles, CA 90095.

[6]Division of Dermatology, Department of Medicine, UCLA David Geffen School of Medicine; Los Angeles, CA 90095.

[7]Division of Hematology and Oncology, UCLA David Geffen School of Medicine; Los Angeles, CA 90095.

[8]Division of Endocrinology and Diabetes, USC Keck School of Medicine; Los Angeles, CA 90033.

[9]Division of Pediatric Endocrinology, UCLA David Geffen School of Medicine; Los Angeles, CA 90095.

Abstract

Autoimmune toxicity occurs in up to 60% of patients treated with immune checkpoint inhibitor (ICI) therapy for cancer and represent an increasing clinical challenge for expanding the use of

*Corresponding author: Melissa G. Lechner, Division of Endocrinology, Diabetes, and Metabolism, UCLA David Geffen School of Medicine; 10833 Le Conte Ave, CHS 52-262, Los Angeles, CA. MLechner@mednet.ucla.edu.
†These authors contributed equally to this work.

Author contributions:
M.G.L., A.D., A.R., T.E.A., M.A.S. conceptualized the study. M.G.L., W.H., A.R., T.E.A., and M.A.S. developed the methodology and clinical protocol. M.G.L., Y.Z., A.Y.P., R.Y.T, H.C., W.H. performed scRNAseq and clonotype analyses. M.G.L., A.I.H., N.H., J.O., L.N.S. performed mouse experiments. M.G.L., A.I.H., J.O., N.H., L.N.S., R.Y.T., K.K. performed in vitro assays and flow cytometry. M.G.L., P.F., T.E.A. performed thyroid FNAs. M.G.L., Y.Z., H.C., A.Y.P., M.A.S. contributed to data visualization. M.G.L. and M.A.S. supervised the work. M.G.L., Y.Z., N.H., L.N.S., A.Y.P. contributed to the original draft. J.O., W.H., H.C., A.D., T.E.A., P.F., A.R., M.A.S reviewed and edited the final manuscript.

List of Supplementary Materials
Materials and Methods
Fig. S1 to S5
Tables S1 to S3
Data files S1 to S3
References (71–74)

these treatments. To date, human immunopathogenic studies of immune related adverse events (IRAEs) have relied upon sampling of circulating peripheral blood cells rather than affected tissues. Here, we directly obtained thyroid specimens from individuals with ICI-thyroiditis, one of the most common IRAEs, and compared immune infiltrates to those from individuals with spontaneous autoimmune Hashimoto's thyroiditis (HT) or no thyroid disease. Single cell RNA sequencing revealed a dominant, clonally expanded population of thyroid-infiltrating cytotoxic $CXCR6^+$ $CD8^+$ T cells (effector $CD8^+$ T cells) present in ICI-thyroiditis, but not HT or healthy controls. Furthermore, we identified a crucial role for interleukin (IL)-21, a cytokine secreted by intrathyroidal T follicular (Tfh) and T peripheral helper (Tph) cells, as a driver of these thyrotoxic effector $CD8^+$ T cells. In the presence of IL-21, human $CD8^+$ T cells acquired the activated effector phenotype with upregulation of the cytotoxic molecules interferon (IFN)-g and granzyme B, increased expression of the chemokine receptor CXCR6, and thyrotoxic capacity. We validated these findings in vivo using a mouse model of IRAEs, and further demonstrated that genetic deletion of IL-21 signaling protected ICI-treated mice from thyroid immune infiltration. Taken together, these studies reveal mechanisms and candidate therapeutic targets for individuals who develop IRAEs.

One Sentence Summary:

Cytotoxic IFN-γ^+ $CXCR6^+$ effector $CD8^+$ T cells and IL-21^+ $CD4^+$ T helper cells contribute to the pathogenesis of checkpoint inhibitor thyroiditis.

INTRODUCTION

Immune checkpoint inhibitors (ICI) targeting programmed death protein 1 (PD-1), programmed cell death ligand 1 (PD-L1), and cytotoxic T lymphocyte antigen (CTLA-4) have dramatically improved outcomes for many patients with advanced malignancies (1). But with increased immune activation can come unwanted autoimmune attack on healthy tissues. Such immune related adverse events (IRAEs) occur in up to 60% of patients treated with ICI therapy for cancer and can contribute to treatment interruption, hospitalizations, and even premature death (2, 3). With the expanding use of ICI therapy (4), IRAEs represent an increasing clinical problem.

The thyroid is one of the most common organs affected by ICI-associated autoimmunity, targeted in approximately 10 to 15% of patients treated with anti-PD-1/PD-L1 monotherapy and nearly 30% of patients treated with anti-PD-1/PD-L1 and anti-CTLA-4 combination therapy (5–7). ICI-induced thyroid autoimmunity, or thyroiditis, presents as immune infiltration and rapid destruction of the thyroid gland, leading to hormone abnormalities and requiring lifelong thyroid hormone replacement in most patients (5, 6, 8). Despite multiple efforts to date, the cause of many IRAEs remain poorly understood, including ICI-thyroiditis. Recent mechanistic studies by us and others showed a key role for T cells and interleukin (IL)-17A in ICI-thyroiditis in mouse models (9–11). It remains unclear, however, whether these findings translate to human IRAEs, which highlights the need for evaluating IRAE immunopathogenesis in humans.

Like IRAEs in other organs, ICI-thyroiditis has both overlapping and distinct features with spontaneous autoimmunity, such as Hashimoto's thyroiditis (HT) (6–8, 12). HT is a common form of thyroid autoimmunity present in nearly 10% of the US population. HT is characterized by slowly progressive thyroid gland immune cell-mediated destruction (13). Central to the pathogenesis of HT are Type 3 immune responses, namely IL-17 producing $CD4^+$ T helper cells (14–17). In addition, tertiary lymphoid follicular structures are classically seen in thyroid immune infiltrates in HT (18), in conjunction with increased circulating T follicular helper (Tfh) cells compared to healthy controls (19). Two prior studies (20, 21) showed intrathyroidal lymphocyte accumulation in the thyroid tissue of patients with ICI-thyroiditis, similar to HT.

On the other hand, ICI-thyroiditis has several notable differences from HT. In contrast to spontaneous HT, thyroid gland destruction in ICI-thyroiditis is more rapid, occurring over weeks rather than years (6, 8). Furthermore, approximately half of patients with ICI-thyroiditis lack the hallmark anti-thyroid antibodies present in HT (6, 8). Thus, ICI-thyroiditis, while likely sharing some overlapping mechanisms with HT, may also be driven by additional distinct immune mechanisms.

To develop strategies to reduce ICI autoimmune toxicities in patients, driving mechanisms need to be identified. Studies into the immunopathogenesis of IRAEs in humans have largely relied upon sampling of peripheral blood rather than affected tissues (22–25). Direct evaluation of immune infiltrates in IRAE tissues, however, may better elucidate pathogenic mechanisms driving autoimmunity (26–29). Therefore, to delineate human IRAE pathogenesis, we sampled thyroid tissue from individuals with ICI-thyroiditis and compared them to those from individuals with HT and healthy controls. Using single cell RNA sequencing of human thyroid fine needle aspiration (FNA) specimens, we identify activated $CXCR6^+$ interferon (IFN)-γ^+ cytotoxic effector $CD8^+$ T cells as key contributors to ICI-thyroiditis. In addition, we identify a mechanism by which IL-21, an important cytokine secreted by Tfh and T peripheral helper (Tph) cells, can promote differentiation of these thyrotoxic effector $CD8^+$ T cells. This role of IL-21^+ Tfh and Tph cells, which were present in both HT and ICI-thyroiditis, suggests a potential link between underlying thyroid autoimmunity and the development of thyroid IRAEs. Finally, we corroborate these findings in vivo using a mouse model of ICI-associated autoimmunity and show that genetic deletion of IL-21 receptor signaling reduced cytotoxic $CXCR6^+$ IFN-γ^+ effector $CD8^+$ T cell numbers and thyroid autoimmune infiltrates. Together, these findings demonstrate a key thyrotoxic pathway in which IL-21^+ Tfh and Tph cells drive cytotoxic effector $CD8^+$ T cell development in ICI-thyroiditis.

RESULTS

Thyroid-infiltrating immune populations in ICI-thyroiditis patients are T cell-predominant and include IL-21^+ $CD4^+$ Tfh and Tph cells.

T cells are presumed mediators of ICI-related autoimmunity. However, these conclusions are based largely on data derived from circulating immune populations, inferences from anti-tumor immune responses, or preclinical models (1, 9, 10, 22–24, 30, 31). Direct data from affected tissues of patients with IRAEs have been limited (20, 21). Therefore, to

better understand the mechanisms driving IRAEs in humans, we evaluated immune cells in thyroid specimens from patients with ICI-thyroiditis (IRAE, n=9 patients) (Fig. 1A). IRAE patients included recipients of combination anti-PD-1 and anti-CTLA-4 therapy, anti-PD-1 monotherapy, or anti-PD-L1 monotherapy for non-thyroid, solid malignancies and developed newly abnormal thyroid function tests consistent with thyroiditis (suppressed TSH and elevated FT4). Thyroid FNAs were collected within 2 months of the first abnormal thyroid function tests and thyroid autoantibodies (anti-thyroglobulin or anti-thyroid peroxidase) were present in 4 of 9 patients. Full clinical and demographic parameters for patients are shown in table S1.

Given the small number of cells present in thyroid specimens (approximately 10,000 cells per aspirate), we first sought to ascertain that immune cells could be detected within these samples. Flow cytometry analysis showed that immune cells were indeed present, and that T cells, including $CD4^+$ and $CD8^+$ subsets, were the primary immune cell subset in ICI-thyroiditis (Fig. 1B and 1C), consistent with a prior report by Kotwal *et al.* evaluating thyroid IRAEs (20). We then turned to single cell RNA sequencing (scRNAseq) for a more detailed characterization of immune infiltrates (Fig. 1D). $CD45^+$ thyroid infiltrating immune cells were sorted from thyroid specimens (n=5 IRAE patients) and subjected to the 10x Genomics scRNAseq pipeline. Uniform Manifold Approximation and Projection (UMAP) visualization revealed 14 distinct groups (fig. S1 and data file S1), representing six broad cell types: $CD4^+$ T cells (*CD3E, CD4*), $CD8^+$ T cells (CD8: *CD3, CD8A, CD8B*), B cells (*CD19, CD79A*), myeloid cells (*CD14, CD68, CSF1R*), gamma delta (γδ) T cells (*CD3E, TRDC,* variable *TRGV* genes), and natural killer (NK) cells (*NKG7, NCR1, FGFBP2*) (Fig. 1D). By absolute cell count, $CD4^+$ and $CD8^+$ T cells make up the majority of immune cells infiltrating the thyroid (Fig. 1E; cell counts in data file S2). These data demonstrate that thyroid immune infiltrates in ICI-thyroiditis patients contain diverse immune cells, with T cells as the primary population.

$CD4^+$ T helper cells drive spontaneous thyroid autoimmunity in many tissues (15, 16, 19) and have been implicated in ICI-associated thyroid autoimmunity in mouse models (9, 10, 30). Therefore, we took a closer look at thyroid-infiltrating $CD4^+$ T cells in our scRNAseq data (Fig. 1F). We observed that thyroid infiltrates contained Tfh cells (*PDCD1*$^+$ *ICOS*$^+$ *BCL6*$^+$ *CXCR5*$^{+>}$) and Tph cells (*PDCD1*$^+$ *ICOS*$^+$ *CXCR5*$^-$ *PRDM1*$^+$), populations that have been associated with multiple spontaneous autoimmune diseases, including HT (19, 32–35). Tfh and Tph cells classically recruit B and T cells through chemokine CXCL13 and produce IL-21 to promote B cell antibody production (33, 34) (Fig. 1F). In addition, recent data suggested that IL-21 from Tfh may drive increased pathogenicity of $CD8^+$ T cells in anti-viral and anti-tumor immune responses (36–38).

Comparison to Hashimoto's thyroiditis reveals expansion of $CD8^+$ T cells in ICI-thyroiditis.

Based upon the presence of $CD4^+$ Tfh and Tph in ICI-thyroiditis, populations previously associated with spontaneous autoimmunity, we sought to probe the relationship between ICI-thyroiditis and HT. Using scRNAseq, we compared thyroid immune infiltrates in ICI-thyroiditis patients (n=5) to those with HT (n=5), as well as controls with no thyroid disease (Healthy Control; n=3, pooled). HT patients were defined as having thyroid

autoantibodies, ultrasound imaging changes consistent with chronic lymphocytic thyroiditis, and biochemical hypothyroidism or treatment with levothyroxine (table S1). Healthy controls were biochemically and clinically euthyroid, had no thyroid autoantibodies, and normal thyroid ultrasound appearance.

We integrated scRNAseq data from IRAE, HT, and healthy control thyroid specimens and visualized the data by UMAP. Clustering of $CD45^+$ intrathyroidal immune cells again showed diverse immune populations, with 13 distinct clusters that were represented across all conditions (Fig. 2A; differentially expressed genes in Fig. 2B and data file S1; cell counts in data file S2). Similar to ICI-thyroiditis alone, $CD4^+$ (*CD3E, CD4*) and $CD8^+$ T cells (*CD3E*, *CD8A, CD8B)* dominated immune infiltrates (Fig. 2B). Other populations were B cells (*CD19, CD79A*), myeloid cells (*CD14, CD68*), γδ T cells (*CD3E, TRDC,* variable *TRGV* genes), and NK cells (*NKG7, FCGR3A, NCR1*) (Fig. 2B). Importantly, *IL21*$^+$ $CD4^+$ T cells (cluster CD4–4), comprising Tfh and Tph cells, were prominent in thyroid immune infiltrates and present across both HT and ICI-thyroiditis states (Fig. 2A and B). These data are consistent with a prior report by Zhu *et al.* (19) showing increased Tfh in HT, and support a role for *IL21*-expressing $CD4^+$ cells in ICI-thyroiditis. Thus, *IL21*-expressing $CD4^+$ T cells may be a shared mechanism between HT and ICI-thyroiditis.

To identify immune mechanisms unique to IRAEs, we performed differential pathway analysis between HT and ICI-thyroiditis specimens. $CD8^+$ T cell-related pathways, notably $CD8^+$ T cell receptor (TCR) signaling, cytolysis, and IFN-γ response, were increased in ICI-thyroiditis compared to HT (Fig. 2C). Consistent with this, $CD8^+$ T cells were also increased in frequency among thyroid-infiltrating immune cells in ICI-thyroiditis compared to HT (Fig. 2D).

The expansion of specific T cell receptor clonotypes is likely an indicator of antigen recognition and subsequent activation and proliferation among $CD8^+$ T cells. We queried T cell clonal expansion in thyroid immune infiltrates across thyroid states using 10x single cell TCR sequencing of thyroid specimens from individuals with IRAEs (n=5), individuals with HT (n=5), and healthy controls (n=3). Overall T cell clonal expansion was greater in patients with ICI-thyroiditis compared to HT, and no clonal expansion was seen in healthy controls (Fig. 2E). Clonally expanded T cells mapped to multiple $CD4^+$ and $CD8^+$ populations, but the largest clonotype expansion in ICI-thyroiditis was seen in $CD8^+$ T cells (Fig. 2F). Together, these data suggest a more prominent role of clonally-expanded $CD8^+$ T cells in the pathogenesis of ICI-thyroiditis.

ICI-thyroiditis is distinguished from HT by intrathyroidal accumulation of clonally expanded, *CXCR6*-, *GZMB*-, and *IFNG*-expressing effector $CD8^+$ T cells.

To further explore how $CD8^+$ T cells may be contributing to IRAEs, we subsetted out $CD8^+$ T cells from the larger population of thyroid infiltrating $CD45^+$ immune cells and compared gene expression across thyroid conditions. $CD8^+$ T cells in patients with ICI-thyroiditis showed significantly greater expression of *IFNG, GZMB*, *FASLG*, and *CXCR6* than HT or healthy controls (Fig. 3A, $p<0.0001$ for all). These genes drive cell-mediated immunity, cytotoxicity, and T cell homing to inflamed tissues (39–43) – key processes in autoimmune tissue attack. By contrast, genes associated with a progenitor phenotype,

including *TCF7* [encoding t cell factor 1 (Tcf1)] and *SELL*, had lower expression in ICI-thyroiditis (Fig. 3A). These data suggest that effector $CD8^+$ T cells are a critical component of ICI-thyroiditis and distinguish this disease entity from other thyroid states.

We subclustered $CD8^+$ T cells to better define the specific populations comprising autoimmune infiltrates in the thyroid. Intrathyroidal $CD8^+$ T cells were comprised of five distinct groups (Fig. 3B, and data file S1), defined as progenitor (Cluster 1; *SELL, TCF7*), memory $IL7R^+$ (Cluster 2; *IL7R, SELL, TCF7*), $EOMES^+$(Cluster 3; *EOMES*), $CXCR6^+$ (Cluster 4; *CXCR6, IFNG, GZMB*) or $TIGIT^+$ (Cluster 5; *TIGIT, LAG3*). Subclustering revealed a population of $CD8^+$ T cells in Cluster 4 with a gene signature that mirrored the differentially expressed genes in $CD8^+$ T cells from ICI-thyroiditis versus HT and HC, namely $CXCR6^+ GZMB^+ FASLG^+ PDCD1^+$ and $TCF7^-$ (Fig. 3C). Furthermore, the cells in Cluster 4 matched the phenotype of "$CD8^+$ autoimmune mediators" that have recently been associated with autoimmunity. Gearty *et al.* (44) and Ciecko *et al.* (45) both identified IFN-γ^+ granzyme (GZMB)$^+$ $CXCR6^+$ $TCF1^-$ $CD8^+$ T cells as immune effectors contributing to autoimmune tissue attack in the pancreas in mouse models of diabetes mellitus. In addition, Dudek and colleagues reported that cytotoxic $CXCR6^+$ $CD8^+$ autoimmune mediator T cells can drive immune-mediated liver injury (46). However, $CD8^+$ autoimmune mediator T cells have not previously been associated with autoimmune thyroiditis in humans.

Whether these activated effector $CD8^+$ T cells expressing *CXCR6*, *IFN-*γ, and cytotoxicity genes migrate from draining lymph nodes or develop within inflamed tissues is unclear (44, 45). To define the ontogeny of these effector $CD8^+$ T cells, we examined transcriptional transitions among intrathyroidal $CD8^+$ subsets. Trajectory analysis showed that $CD8^+$ T cells progressed along a single lineage from progenitors to cytotoxic effectors (Fig. 3D). Specifically, $CD8^+$ cells decreased expression of *TCF7* and *SELL* and increased expression of *IFNG, GZMB, FASLG*, and *CXCR6* along the trajectory (Fig. 3E). This is most consistent with the findings from Ceicko *et al.* (45) in diabetes showing that progenitor $CXCR6^- TCF7^+$ $CD8^+$ T cells give rise to pathogenic $CXCR6^+ TCF7^-$ $CD8^+$ autoimmune mediator T cells in the tissue and that these progeny are sufficient to cause autoimmunity. Thus, activated cytotoxic effector $CD8^+$ T cells expressing $CXCR6^+$ and *IFN-*γ^+ in human thyroiditis likely arise from intrathyroidal progenitors through a differentiation pathway that may be shared across autoimmune diseases.

Importantly, intrathyroidal $CD8^+$ T cell differentiation was distinct across thyroid states. In ICI-thyroiditis patients, the majority of $CD8^+$ T cells showed differentiation to mature $CD8^+$ effectors ($CXCR6^+ GZMB^+ IFNG^+ TCF7^-$) (Fig. 3F). In contrast, $CD8^+$ T cells in healthy controls remained primarily in the progenitor or exhausted $TIGIT^+ PD1^+$ subsets, whereas $CD8^+$ T cells in HT patients were most likely in the $EOMES^+$ cluster as precursors to the fully activated cytotoxic effector population. Consistent with these data, ICI-thyroiditis patients had a greater frequency of $CXCR6^+ IFNG^+ GZMB^+$ effector $CD8^+$ T cells (Cluster 4) in thyroid immune infiltrates than HT patients (Fig. 3G, $p<0.05$).

TCR clonal expansion, an indicator of antigen recognition and response within $CD8^+$ T cell populations, was greatest within the $CXCR6^+ IFNG^+ GZMB^+$ effector $CD8^+$ T cells (Cluster 4) (Fig. 3H), further supporting their participation in thyroid tissue autoimmune

attack. In addition, greater clonotype expansion correlated with increasing expression of cytotoxic and effector (*GZMB, IFNG*, *CXCR6*) and checkpoint protein (*PDCD1, CTLA4, LAG3*) genes (fig. S2A), although no increased proliferation was observed (fig. S2B). Shared clonotypes across clusters also serve as lineage markers as cells undergo transcriptional transitions. Clonally expanded *CXCR6*$^+$ *IFNG*$^+$ *GZMB*$^+$ effector CD8$^+$ T cells (Cluster 4) had shared clonotypes with cells across the *EOMES*$^+$ (Cluster 3) and *TIGIT*$^+$ (Cluster 5) subsets (fig. S2C), and the clonal transition index was highest across these three clusters (fig. S2D). Taken together, this supports the notion that *CXCR6*$^+$ *IFNG*$^+$ *GZMB*$^+$ effectors may arise from activation and differentiation of intrathyroidal T cells upon ICI treatment. Thus, our data show a relationship between clonal expansion and acquisition of cytotoxic effector function by CD8$^+$ T cells in thyroid immune infiltrates. In summary, activation and differentiation of clonally-expanded CD8$^+$ T cells to cytotoxic *CXCR6*- and *IFNG*-expressing effectors in the thyroid is a distinguishing feature of ICI-thyroiditis.

IL-21 promotes the CD8$^+$ T cell effector mediator phenotype

Our initial observations in IRAE samples showed prominent *IL21*-expressing CD4$^+$ Tfh and Tph cells in thyroid immune infiltrates (Fig. 1D). How CD4$^+$ Tfh and Tph cell population dynamics change between IRAE, HT, and healthy controls, however, remain unclear. Using our integrated dataset of thyroid-infiltrating immune cells from individuals with IRAEs, individuals with HT, and healthy controls, we isolated and subclustered the CD4$^+$ T cells. We delineated thyroid-infiltrating CD4$^+$ T cell subsets across thyroid conditions, yielding eight distinct populations (Fig. 4A). In addition to three Tfh and Tph clusters [Tfh-1 (*ICOS, CXCL13, PDCD1*), Tfh-2 (*TOX2, ICOS, CXCL13, PDCD1, CXCR5, IL21*) and Tph (*ICOS, PDCD1*)], we also saw *CCR7*$^+$ (*SELL, CCR7, LEF1*), memory *IL7R*$^+$ (*IL7R, SELL*), *IL7R*$^+$ *PD1*$^+$ (*IL7R, PDCD1, CD44*), *CD44*$^+$, and *GZMK*$^+$ groups (Data file S1). Importantly, Tfh and Tph cells expressed *IL21*, *CXCL13*, *PDCD1* and *CTLA4* (Fig. 4B). Furthermore, trajectory analysis showed that differentiation from *IL7R*- and *PD1*-expressing and *CCR7*-expressing cells to Tph was significantly increased in ICI-thyroiditis compared to HT and healthy controls (Fig. 4C, left, $p<0.0001$). Differentiation from *IL7R*$^+$*PD1*$^+$ and *CCR7*$^+$ cells to Tfh cells was increased in both ICI-thyroiditis and HT compared to healthy controls (Fig. 4C, $p<0.0001$). Thus, differentiation toward *IL21*$^+$ CD4$^+$ Tph and Tfh cells was increased within the thyroid tissue in ICI-thyroiditis patients, indicating their potential importance to IRAE immunopathogenesis.

Recent data show that, aside from its established role in promoting B cell responses, IL-21 can promote CD8$^+$ T cell pathogenicity (36–38). These data led us to hypothesize that IL-21 produced by Tfh and Tph may be promoting CD8$^+$ T cell differentiation toward cytotoxic effectors in ICI-thyroiditis (Fig. 4D). Indeed, in vitro stimulation with anti-CD3/28 and recombinant IL-21 increased expression of the cytotoxic molecule granzyme B and the chemokine receptor CXCR6 in human CD8$^+$ T cells, compared to anti-CD3/28 alone (Fig. 4E). IL-21-induced CXCR6$^+$ CD8$^+$ T cells also expressed checkpoint proteins PD-1 and CTLA-4 (fig. S3A), similar to autoimmune mediators described by Ciecko *et al.* (45) and Dudek *et al.* (46). Thus, IL-21 promotes differentiation of human CD8$^+$ T cells to become autoimmune mediator-like cells with a CXCR6$^+$ GZMB$^+$ PD-1$^+$ CTLA-4$^+$ phenotype.

Despite their expression of cytotoxic molecules and effector molecules, it remains unclear whether IL-21-induced $CD8^+$ T cells are thyrotoxic. For these studies, we incubated human thyroid cells (NThyOri3.1 cell line) with supernatants from IL-21-stimulated human $CD8^+$ T cells. Importantly, incubation with supernatants from IL-21 + anti-CD3/28-stimulated $CD8^+$ T cells resulted in greater killing of human thyroid cells compared to supernatants from anti-CD3/28-treated $CD8^+$ T cells or unstimulated $CD8^+$ T cells (fig. S3B). Thus, IL-21 from Tfh and Tph cells can drive human $CD8^+$ T cells to become thyrotoxic effectors.

ICI treatment in an IRAE mouse model recapitulates expansion of $CXCR6^+$ IFN-γ^+ $CD8^+$ effectors and IL-21^+ $CD4^+$ Tfh and Tph cells

Our data from human thyroid specimens revealed a mechanism by which IL-21 from Tfh and Tph cells contributes to the development of ICI-thyroiditis through the expansion of thyrotoxic *CXCR6*$^+$ *IFNG*$^+$ $CD8^+$ effector T cells. To further explore this mechanism in vivo, we turned to our recently developed IRAE mouse model (9) (Fig. 5A). In this model, autoimmunity-prone non-obese diabetic (NOD) mice treated with anti-PD-1 and anti-CTLA-4 monoclonal antibodies develop multi-organ autoimmunity, including thyroiditis. Similar to patients treated with ICI for cancer therapy, mice developed autoimmunity more frequently with the combination of anti-PD-1 + anti-CTLA-4 (Dual ICI) versus with single agent ICI treatment. In our model, $CD8^+$ effector ($CXCR6^+$ $GZMB^+$ IFN-γ^+) T cells were increased in ICI-treated NOD mice as compared with isotype controls in both tumor models evaluated (Fig. 5B). Additionally, ICI-treated mice had increased Tfh [$CXCR5^-$ $PD\text{-}1^+$ Inducible T-cell costimulator $(ICOS)^+$ $CD4^+$] and Tph ($CXCR5^-$ $PD\text{-}1^+$ $ICOS^+$ $CD4^+$) cells (Fig. 5C) and greater IL-21 production by helper T cells (Fig. 5D). These findings recapitulate the finding that ICI treatment is associated with expansion of *CXCR6*$^+$ *IFNG*$^+$ *GZMB*$^+$ $CD8^+$ effector T cells and *IL21*$^+$ $CD4^+$ Tfh and Tph populations in humans. In summary, our data show that in an in vivo mouse model, there is an increase in IL-21-producing Tfh and Tph cells and $CXCR6^+$ IFN-γ^+ $GZMB^+$ $CD8^+$ effector T cells during ICI therapy.

Deficiency in IL-21 signaling reduces $CXCR6^+$ $CD8^+$ effector T cells and protects ICI-treated mice from thyroid autoimmune infiltrates.

Taken together, our data suggested a role for an IL-21-producing Tfh and Tph cell – $CD8^+$ T effector T cell axis in the development of ICI-thyroiditis. Congruent with our findings in humans, recombinant IL-21 increased expression of effector molecules GZMB and IFN-γ (Fig. 6A) as well as increased expression of CXCR6 (Fig. 6B) by murine $CD8^+$ T cells in vitro. Based upon these data, we predicted that genetic elimination of IL-21 signaling in our mouse model could reduce thyroid immune infiltrates during ICI treatment (Fig. 6C).

We compared autoimmune infiltrates mice with genetic deletion of the gene encoding the IL-21 receptor (NOD.*Il21r*$^{-/-}$; IL-21R KO) to wild type (WT) controls during ICI treatment (Fig. 6D). Indeed, the frequency of $CXCR6^+$ $CD8^+$ T cells was reduced in ICI-treated IL-21R KO mice compared to ICI-treated WT mice (Fig. 6E, p=0.0057). Furthermore, IL-21R KO mice were protected from ICI-associated thyroid autoimmunity compared to WT controls (Fig. 6F). After 4 weeks of anti-PD-1 + anti-CTLA-4 treatment, thyroid-infiltrating $CD45^+$ and $CD3^+$ immune cells were reduced in IL-21R KO mice compared to

ICI-treated WT mice, and similar to isotype treated WT controls (Fig. 6F, p=0.0057 and p=0.0016, respectively). Thus, deletion of IL-21 signaling during ICI treatment reduced ICI-associated thyroid autoimmune infiltration. These data suggest that IL-21-induced immune effectors play a crucial role in the development of ICI-thyroiditis.

T cell IL-21 signaling drives ICI-associated thyroid autoimmunity.

Based upon our human scRNAseq and mouse data, we predicted that IL-21 action on T cells was a primary driver of ICI-thyroiditis. However, IL-21 is a pleiotropic cytokine with action on multiple immune populations. IL-21 targets $CD4^+$ T cells to promote the further differentiation of $IL\text{-}21^+$ producing Tfh and Tph cells, as well as $IL\text{-}17^+$ producing T helper cells (Th17). Both Tfh/Tph and Th17 T cells have been associated with spontaneous autoimmune disease, and more recently IRAEs (9, 23, 24). In $CD8^+$ T cells, IL-21 also enhanced cytotoxicity and effector function. In addition to its actions on T cells, IL-21 plays an important role in B cell proliferation and antibody production and class switching (33, 35); it can also enhance phagocytosis by macrophages (47).

We used ICI treatment of NOD mice with genetic deletion of the TCR alpha gene (NOD.*Tcra*$^{-/-}$; TCRα KO), which fail to develop mature $CD4^+$ and $CD8^+$ T cells, to test whether T cells are required for the development of ICI-thyroiditis. Consistent with previous prior reports, TCRα KO mice were protected from thyroiditis during ICI treatment (fig. S4) (10). We next reconstituted immune deficient NOD.SCID mice (which lack T and B cells) with $CD4^+$ and $CD8^+$ T cells from WT NOD mice, and then treated them with either ICI or isotype control antibodies for four weeks (Fig. 6G). Transfer of WT $CD4^+$ and $CD8^+$ T cells into NOD.SCID mice was sufficient to induce thyroiditis in ICI-treated mice; 5 of 7 mice (71%) developed thyroid immune infiltrates by 4 weeks (Fig. 6H). However, only 1 of 7 (14%) NOD.SCID mice reconstituted with IL-21R KO $CD4^+$ and $CD8^+$ T cells developed thyroiditis with ICI treatment (Fig. 6H). These data demonstrate that IL-21R signaling on $CD4^+$ and $CD8^+$ T cells promotes the development of ICI-thyroiditis, and may be a therapeutic target for the prevention of IRAEs in humans.

DISCUSSION

Autoimmune toxicities remain an important limitation to the benefits and use of ICI cancer therapy. Despite multiple efforts to date, strategies to reduce IRAEs have been elusive, in part due to a lack of understanding of pathogenic immune cells within the tissue microenvironment. In this study, we report for the first time the intrathyroidal immune composition of autoimmune infiltrates in human ICI-thyroiditis, one of the most common IRAEs in patients, using scRNAseq and TCR seq. Intrathyroidal infiltrates were T cell-predominant and included IL-21-producing $CD4^+$ Tfh and Tph populations. Comparisons to HT and healthy control samples revealed a predominant, clonally expanded activated $CD8^+$ T cell population expressing CXCR6, IFN-γ, and cytotoxicity genes in individuals with ICI-thyroiditis. Expansion of this $CD8^+$ effector population was recapitulated in an IRAE mouse model. Finally, our data show that $CXCR6^+$ activated $CD8^+$ effector differentiation and thyroiditis development were dependent on IL-21, since genetic deletion of IL-21R prevented their differentiation and protected mice from ICI-associated thyroiditis.

CD8$^+$ autoimmune mediators with this cytotoxic and CXCR6$^+$ IFN-g$^+$ phenotype a have recently been shown to drive pathogenic immune responses in preclinical models of autoimmune diabetes and hepatitis (44–46). These cells differentiate from stem-like progenitors in lymph nodes or within the tissue to become terminal effectors with cytotoxic function. During this transition, CD8$^+$ effectors down regulate Tcf1 and increase expression of CXCR6, IFN-γ, GZMB, PD-1 and CTLA-4. This autoimmune mediator population is emerging as a common effector phenotype shared across autoimmunity in different tissues. We now extend the role of CD8$^+$ autoimmune mediators to ICI-thyroiditis in both humans and mice. In support of a pathogenic role in ICI-thyroiditis, thyroid-infiltrating autoimmune mediators acquire cytotoxic gene expression in conjunction with TCR clonal expansion, likely consistent with thyroid antigen response. Furthermore, *CXCR6*$^+$ *IFNG*$^+$ cytotoxic effector CD8$^+$ T cells expressed *PDCD1* (encoding PD-1) and *CTLA4* and therefore may be direct targets of ICI antibody binding. In contrast to HT, where T cells are kept in check by T cell PD-1 binding to thyroid cell PD-L1 (48), in IRAEs, autoreactive CD8$^+$ T cells may be released from checkpoint inhibition during ICI therapy. Furthermore, the greater CD8$^+$ effector activation seen in ICI-thyroiditis, as compared with HT, may underlie the much more rapid clinical progression of gland inflammation and destruction that is a hallmark of many IRAEs in comparison to their spontaneous autoimmune disease counterparts (6, 49).

Evidence for CD8$^+$ T cell enrichment in human IRAEs was also seen in recent studies by Sasson *et al.* (27) and Luoma *et al.* (29), in which increased IFN-γ^+ CD8$^+$ T cells were seen in patients with ICI-related colitis. Ongoing studies are interrogating these TCR sequences of clonally expanded CD8$^+$ effectors to determine antigen targets in thyroid IRAEs. Clonal expansion of T cells has been linked to IRAE risk in several recent studies (22, 26, 29), including clonal expansion of CD8$^+$ T cells in patients with ICI-colitis (29) and in a mouse model of ICI-associated myocarditis (26). Importantly, whether clonal expansion also occurs in human ICI-associated myocarditis is unknown, as this study did not evaluate immune infiltrates in the tissues of ICI-myocarditis patients. Thus, in addition to ICI-thyroiditis, cytotoxic CXCR6$^+$ IFN-γ^+ CD8$^+$ effectors may be central to IRAEs in other tissues, and more investigations at the tissue level in humans are needed.

Interestingly, effector CD8$^+$ T cells with a similar phenotype have also been seen within intratumoral infiltrates in ICI-treated cancer patients (50–52). Across patients with multiple types of cancer, Rosenberg and colleagues identified clonally-expanded, tumor-antigen specific effector CD8$^+$ T cells as a subset with high *CXCR6, GZMB, PRF1*, *CXCL13*, and *TOX* gene expression (50–52). In addition, Thommen *et al.* (53) reported improved survival in lung cancer patients treated with ICI who had greater tumor infiltration by a subset of CD8$^+$ PD-1^{high} T cells expressing *CXCR6*, *GZMB*, and *IFNG*. Thus, these activated CD8$^+$ effector T cells are emerging as an important player in both IRAEs and perhaps ICI anti-tumor responses. In fact, development of ICI-thyroiditis is associated with a survival benefit and improved response to ICI therapy (54, 55). Further studies to understand the interplay between thyroid IRAEs and anti-tumor responses may help to improve ICI efficacy.

Our data also suggest a role for IL-21$^+$ CD4$^+$ Tfh and Tph cells in the development of ICI-thyroiditis and as a shared mechanism with HT. This may explain why patients with

pre-existing thyroid autoantibodies are at a higher risk of developing thyroid IRAEs during ICI therapy (56). Wherry and colleagues recently showed increased chemokine expression (CXCL13) and B cell co-stimulation by circulating Tfh cells in anti-PD-1 treated patients compared to untreated individuals (24). In this study, we show that both Tfh and Tph cells infiltrate into IRAE-affected thyroid tissue and propose a mechanism by which Tfh and Tph cells may contribute to autoimmunity during ICI therapy through IL-21 action on $CD8^+$ T cells. Specifically, recombinant IL-21 drove differentiation of activated $CD8^+$ effectors in vitro expressing CXCR6, GZMB, and IFN-γ and increased thyrotoxic activity, suggesting it as a potential target to reduce IRAEs.

Of note, IL-21^+ Tfh and Tph cells can also promote B cell proliferation and antibody production (33, 34). B cells were present in thyroid immune infiltrates of IRAE patients (Fig. 1A), but only about 40% of patients with ICI-thyroiditis have antibodies against thyroid autoantigens thyroid peroxidase (TPO) or thyroglobulin (Tg) (8). In addition, such antibodies did not correlate with thyroid immune infiltrates in two preclincial models of ICI-associated thyroiditis (9, 10).

Our data do not suggest a major contribution from IL-21 signaling to B cells in ICI-thyroiditis; $CD4^+$ and $CD8^+$ T cells were both required and sufficient for the development of thyroid immune infiltrates in ICI-treated mice and genetic blockade of IL-21 signaling in T cells reduced thyroid autoimmunity during ICI therapy.

We acknowledge several limitations of this study. First, the scRNAseq data presented for patients with ICI-thyroiditis encompasses human variation, including differences in primary cancer type, age and sex, and treatment history. In addition, thyroid FNA specimens yield a small number of cells from each participant and therefore confirmatory flow cytometry, which may provide more quantitative data, was not feasible for all specimens. However, these studies do provide the first in depth look into the tissue immune infiltrates of ICI-thyroiditis at greater resolution than prior flow cytometry or immunohistochemistry studies (20, 21). Furthermore, in vitro immune assays with human cells and in vivo studies using a mouse model of IRAEs serve to corroborate the mechanisms inferred from our transcriptional data. We recognize that preclinical models have inherent limitations in their ability to simulate human disease. ICI treatment of NOD mice recapitulates important aspects of the ICI-autoimmune toxicity seen in humans, including multi-organ immune infiltrates (49, 57–60), increasing toxicity with combination versus monotherapy (3, 5), and a similar genetic basis for IRAE susceptibility (61–66). However, the pattern of IRAEs in our mouse model does not align completely with that seen in patients. For example, a lower incidence of skin and liver autoimmunity and an increased risk of diabetes mellitus are seen in the mouse model. In addition, further studies in patients who develop IRAEs and syngeneic mouse tumor models are needed to understand the linkage of IL-21-mediated autoimmunity with anti-tumor responses.

In conclusion, we provide evidence for a diverse immune infiltrate in ICI-associated thyroid autoimmunity and a central role for $CD8^+$ $CXCR6^+$ IFN-γ^+ cytotoxic T cells. As a strategy to reduce autoimmune toxicity, we further identify a supporting role of IL-21 producing $CD4^+$ Tfh and Tph cells through promotion of this effector phenotype in $CD8^+$

T cells. Importantly, as suggested by preclinical data in our mouse model of ICI-associated autoimmunity, targeted blockade of IL-21 signaling may provide an avenue to attenuate ICI autoimmune toxicities.

MATERIALS AND METHODS

Study design

Patients were prospectively enrolled from two academic medical centers (UCLA Health, USC Keck Medical Center) under IRB- approved protocols (21–000633, 19–001708, HS-19–00715). Thyroid FNA specimens were collected from adult (age >18 years) patients with 1) ICI-treated cancer with new onset thyroid IRAE or 2) Hashimoto's thyroiditis. Exclusion criteria included pregnancy, history of thyroid surgery, radioactive iodine therapy, or thyroid cancer, immune modifying conditions not including solid malignancy (e.*g.* bone marrow transplantation, leukemia or lymphoma, known genetic or acquired immunodeficiency, or immune modifying medications at the time of specimen collection, excluding physiologic steroids). ICI-thyroiditis was defined as new onset thyroid dysfunction (within 2 months of specimen collection) while on anti-PD-1, anti-PD-L1,or anti-CTLA-4 monotherapy or while on combination ICI therapy, with an overt hyperthyroid phase (low TSH and elevated FT4) followed by hypothyroidism (elevated TSH and low FT4) requiring thyroid hormone replacement. ICI-treated individuals must have received an FDA-approved ICI within the past 1 month. HT patients had hypothyroidism (elevated TSH and low FT4, or requirement for thyroid hormone replacement) and evidence of thyroid autoimmunity (e.*g.* thyroid autoantibody presence, anti-TPO or anti-Tg); imaging findings, if available, were consistent with HT. Patients may have had a cytologically-proven benign thyroid nodule. Patient demographic, treatment and clinical immune data are summarized in table S1. Thyroid FNA specimens were collected into RPMI-1640 media under ultrasound guidance using 4 passes with a 25 or 27 gauge needle by M.G.L, T.E.A., or P.F. Raw, individual-level data associated with figures are available in Data file S3.

Single cell RNA sequencing

For scRNAseq of human thyroid FNA specimens, single cell suspensions were stained with fluorescence-conjugated antibodies to CD45 and 4′,6-diamidino-2-phenylindole (DAPI). Single live $CD45^+$ immune cells were collected and sorted, then submitted for 10× 5' and TCR sequencing. Specimens with inadequate cell viability were not sequenced. Cell preparation, library preparation, and sequencing were carried out according to Chromium product-based manufacturer protocols (10X Genomics). Sequencing was carried out on a Novaseq6000 S2 2×50bp flow cell (Illumina) utilizing the Chromium single-cell 5′ and TCR gene expression library preparation (10X Genomics), per manufacturer's protocol at the Cedars Sinai Medical Center Genomics Core. Data processing, clustering, differential gene expression and marker identification, trajectory and clonotype analyses are detailed in supplemental materials and methods.

In vitro assessment of primary human immune cells

Peripheral blood mononuclear cells (PBMC) were isolated from blood by density gradient centrifugation (Ficoll-Hypaque). $CD8^+$ T cells were separated by magnetic bead separation

(Miltenyi Biotec). For T cell stimulation assays, PBMC or isolated T cells were cultured at 5×10^5 cells/well in 12 well plates in complete media with 2beta-mercaptoethanol (2ME). Stimulation was provided by human anti-CD3/CD28 Dynabeads (Invitrogen) and recombinant human IL-21 at 100ng/mL (PeproTech) or vehicle control, as indicated. Isolated $CD8^+$ T cells were additionally cultured in the presence of recombinant IL-2 at 50 units/mL. Cytokines were refreshed at day 3 and cells were analyzed by flow cytometry on day 5. Experiments were repeated at least twice.

To test the effect of T cell supernatants on thyroid cell viability, NThy-Ori 3.1 cells were cultured with day 3 supernatant from human $CD8^+$ T cell in vitro cultures diluted 1:1 with fresh complete media. Cell viability was evaluated by staining with DAPI and analysis by flow cytometry at 24 hours. Experiments were repeated at least twice.

Mouse studies

Animal studies were approved by the University of California Los Angeles Animal Research Committee (Protocol C21–039). NOD/ShiLtJ (NOD, 001976), NOD/*Il21r*$^{-/-}$ (IL-21R KO, 034163), NOD/*Trca*$^{-/-}$ (TCRα KO, 004444), and NOD/SCID (001303) mice were obtained from the Jackson Laboratory. Male and female mice were used in equal proportions. Mice were used at 4 to 6 weeks of age unless otherwise noted. Mice were housed in a specific pathogen-free barrier facility at the University of California Los Angeles. Mice in different experimental groups were co-housed.

Immune checkpoint inhibitor treatment of mice

Mice were randomized to twice weekly treatment with anti-mouse CTLA-4 (clone 9D9, BioXcell BE0164) and PD-1 (clone RPM1–14, BioXcell, BE0146) or isotype control antibodies (2A3, MPC-11; BioXcell BE0089 and BE0086), at 10 mg/kg/dose intraperitoneally (i.p.) for four weeks, as described previously (9). ICIs were from BioXcell. During treatment, mice were monitored daily for activity and appearance, and twice weekly for weight and glucosuria. Mice developing glucosuria were treated with 10 units of subcutaneous NPH insulin daily. After four weeks of ICI treatment, mice were euthanized, blood collected by retro-orbital bleed, then perfused with 10mL of phosphate buffered saline (PBS). For evaluation of immune infiltrates by flow, fresh thyroid glands were dissected away from surrounding trachea and lymphoid tissue, digested in collagenase type IV (1mg/mL in 2% fetal bovine serum in PBS) at 37°C for 20 minutes, then mechanically dissociated by passage through a 40μm filter. Spleen cells were isolated by mechanical dissociation and passage through a 40μm filter. Predetermined endpoints for euthanasia before four weeks included >20% weight loss and glucosuria not resolved by insulin therapy, as per IACUC protocols. Immediately after euthanasia and perfusion with sterile PBS, fresh tissues were dissociated for analysis of immune infiltrates by flow cytometry.

Adoptive transfer experiments

Naïve $CD4^+$ and $CD8^+$ T cells from fresh splenocytes from healthy NOD wild type or IL-21R KO mice using magnetic bead separation (EasySep kits). Next, 1×10^6 purified $CD4^+$ and $CD8^+$ T cells were transferred in sterile PBS using retro-orbital injection into immunodeficient, sex-matched NOD.SCID mice. Adoptively transferred mice were then

treated with ICIs or isotype control antibodies for 4 weeks and assessed for the development of autoimmune tissue infiltrates as above.

In vitro assessment of primary murine immune cells

Splenocytes were isolated from healthy NOD.WT mice by mechanical dissociation, and $CD8^+$ T cells were isolated and cultured at 5×10^5 cells/well in 12 well plates in complete media with 2ME. Stimulation was provided by mouse anti-CD3/CD28 Dynabeads (Invitrogen) and recombinant murine IL-21 at 100ng/mL (PeproTech) or vehicle control, as indicated. Cells were evaluated on day 3. Experiments were repeated at least twice.

Flow Cytometry

Methods for staining single cell suspensions are detailed in the supplemental materials and methods, and gating strategies are shown in fig. S5. Antibodies used are detailed in table S2 and table S3. Cell counts are shown as relative frequency of live, gated single cells unless otherwise noted. For determination of infiltrating cells per thyroid lobe, absolute cell counts per thyroid lobe were determined by a calculation of cell count x fraction of thyroid analyzed to estimate a total cell count per thyroid lobe, as done previously (9).

Statistical analysis

Analyses of scRNAseq data were performed in RStudio (v2021.09.2) as described above. Briefly, the Seurat FindMarkers function was used to generate the top upregulated genes for each cluster using a Wilcoxon Rank Sum Test to identify differentially expressed genes across clusters. For gene pathway analysis, significant differential gene expression between conditions was defined as log fold change > 0.5 and P value < 0.05, and evaluated with gene-set enrichment analysis using Metascape (67). For trajectory analysis, to test for significant differences in pseudotime distributions between conditions, asymptotic Kolmogorov-Smirnov tests were conducted between pairwise comparisons across the three conditions (HT, IRAE, and Healthy Control) for each lineage. Differences in clonal expansion and clone overlap between clusters was determined using STARTRAC (68), with differences evaluated by ANOVA with subsequent Tukey's pairwise comparisons. Statistical analyses for all other human and mouse studies were performed with GraphPad Prism software (v9.3.1). Comparisons among multiple groups for continuous data were made using ANOVA or ANOVA with Welch correction with no assumption for equal variances, with subsequent pairwise comparisons by Tukey's or Dunnett's test. Comparisons between two groups were done by two-sided Student's t test with Welch correction with no assumption for equal variances. When multiple comparisons were performed, adjusted p-values are shown. Significance was defined as $\alpha = 0.05$.

Data and materials availability:

All data associated with this study are in the paper or supplementary materials. The datasets for single cell sequencing generated during and analyzed during the current study are available in the Gene Expression Omnibus (GEO) repository under accession number GSE218743 (https://www.ncbi.nlm.nih.gov/geo/).

Supplementary Material

Refer to Web version on PubMed Central for supplementary material.

Acknowledgments:

Funding:

This work was supported by American Thyroid Association grant THYROIDGRANT2020–0000000169 (to MGL), National Institutes of Health grant K08 DK129829–01 (to MGL), and an Aramont Charitable Foundation grant (to MGL).

Competing interests:

A.R. has received honoraria from consulting with Amgen, Bristol-Myers Squibb, Chugai, Genentech, Merck, Novartis, Roche, Sanofi and Vedanta, is or has been a member of the scientific advisory board and holds stock in Advaxis, Appia, Apricity, Arcus, Compugen, CytomX, Highlight, ImaginAb, Isoplexis, Kalthera, Kite-Gilead, Merus, PACT Pharma, Pluto, RAPT, Rgenix, Synthekine and Tango, has received research funding from Agilent and from Bristol-Myers Squibb through Stand Up to Cancer (SU2C), and patent royalties from Arsenal Bio. A.D. has consulted for Bristol-Myers Squibb, AstraZeneca, Radmetrix, Seattle Genetics, Janssen, PACT Pharma, Merck, Roche/Genetech, Exelixis, Dyania Health, and has received research funding Kite/Gilead, AstraZeneca, Roche/Genetech, BMS, Merck, Jounce Therapeutics, Infinity Pharmaceuticals, Seattle Genetics. All other authors declare that they have no competing interests.

References

1. Wei SC, Duffy CR, Allison JP, Fundamental mechanisms of immune checkpoint blockade therapy. Cancer Discov. 8, 1069–1086 (2018). [PubMed: 30115704]
2. Wang DY, Salem JE, Cohen JV, Chandra S, Menzer C, Ye F, Zhao S, Das S, Beckermann KE, Ha L, Rathmell WK, Ancell KK, Balko JM, Bowman C, Davis EJ, Chism DD, Horn L, Long GV, Carlino MS, Lebrun-Vignes B, Eroglu Z, Hassel JC, Menzies AM, Sosman JA, Sullivan RJ, Moslehi JJ, Johnson DB, Fatal Toxic Effects Associated With Immune Checkpoint Inhibitors: A Systematic Review and Meta-analysis. JAMA Oncol. 4, 1721–1728 (2018). [PubMed: 30242316]
3. Larkin J, Chiarion-Sileni V, Gonzalez R, Grob JJ, Rutkowski P, Lao CD, Cowey CL, Schadendorf D, Wagstaff J, Dummer R, Ferrucci PF, Smylie M, Hogg D, Hill A, Márquez-Rodas I, Haanen J, Guidoboni M, Maio M, Schöffski P, Carlino MS, Lebbé C, McArthur G, Ascierto PA, Daniels GA, Long GV, Bastholt L, Rizzo JI, Balogh A, Moshyk A, Hodi FS, Wolchok JD, Five-year survival with combined nivolumab and ipilimumab in advanced melanoma. N. Engl. J. Med 381, 1535–1546 (2019). [PubMed: 31562797]
4. Haslam A, Prasad V, Estimation of the Percentage of US Patients With Cancer Who Are Eligible for and Respond to Checkpoint Inhibitor Immunotherapy Drugs. JAMA Netw. open 2, e192535 (2019). [PubMed: 31050774]
5. De Filette J, Andreescu CE, Cools F, Bravenboer B, Velkeniers B, A Systematic Review and Meta-Analysis of Endocrine-Related Adverse Events Associated with Immune Checkpoint InhibitorsHorm. Metab. Res 51, 145–156 (2019).
6. Iyer PC, Cabanillas ME, Waguespack SG, Hu MI, Thosani S, Lavis VR, Busaidy NL, Subudhi SK, Diab A, Dadu R, Immune-Related Thyroiditis with Immune Checkpoint Inhibitors. Thyroid 28, 1243–1251 (2018). [PubMed: 30132401]
7. Delivanis DA, Gustafson MP, Bornschlegl S, Merten MM, Kottschade L, Withers S, Dietz AB, Ryder M, Pembrolizumab-induced thyroiditis: Comprehensive clinical review and insights into underlying involved mechanisms. J. Clin. Endocrinol. Metab 102, 2770–2780 (2017). [PubMed: 28609832]
8. Ma C, Hodi FS, Giobbie-Hurder A, Wang X, Zhou J, Zhang A, Zhou Y, Mao F, Angell TE, Andrews CP, Hu J, Barroso-Sousa R, Kaiser UB, Tolaney SM, Min L, The impact of high-dose glucocorticoids on the outcome of immune-checkpoint inhibitor–related thyroid disorders. Cancer Immunol. Res 7, 1214–1220 (2019). [PubMed: 31088848]

9. Lechner MG, Cheng MI, Patel AY, Hoang AT, Yakobian N, Astourian M, Pioso MS, Rodriguez ED, McCarthy EC, Hugo W, Angell TE, Drakaki A, Ribas A, Su MA, Inhibition of IL-17A Protects against Thyroid Immune-Related Adverse Events while Preserving Checkpoint Inhibitor Antitumor Efficacy. J. Immunol 209, 696–709 (2022). [PubMed: 35817515]
10. Yasuda Y, Iwama S, Sugiyama D, Okuji T, Kobayashi T, Ito M, Okada N, Enomoto A, Ito S, Yan Y, Sugiyama M, Onoue T, Tsunekawa T, Ito Y, Takagi H, Hagiwara D, Goto M, Suga H, Banno R, Takahashi M, Nishikawa H, Arima H, CD4 + T cells are essential for the development of destructive thyroiditis induced by anti – PD-1 antibody in thyroglobulin-immunized mice. Sci. Transl. Med 7495 (2021).
11. Sharma R, Di Dalmazi G, Caturegli P, Exacerbation of Autoimmune Thyroiditis by CTLA-4 Blockade: A Role for IFNγ-Induced Indoleamine 2, 3-Dioxygenase. Thyroid 26, 1117–1124 (2016). [PubMed: 27296629]
12. De Moel EC, Rozeman EA, Kapiteijn EH, Verdegaal EME, Grummels A, Bakker JA, Huizinga TWJ, Haanen JB, Toes REM, Van Der Woude D, Autoantibody development under treatment with immune-checkpoint inhibitors. Cancer Immunol. Res 7, 6–11 (2019). [PubMed: 30425107]
13. Caturegli P, De Remigis A, Chuang K, Dembele M, Iwama A, Iwama S, Hashimoto's thyroiditis: Celebrating the centennial through the lens of the Johns Hopkins Hospital Surgical Pathology Records. Thyroid 23, 142–150 (2013). [PubMed: 23151083]
14. Miossec P, Korn T, Kuchroo VK, Interleukin-17 and type 17 helper T cells. N. Engl. J. Med 361, 888 (2009). [PubMed: 19710487]
15. Horie I, Abiru N, Nagayama Y, Kuriya G, Saitoh O, Ichikawa T, Iwakura Y, Eguchi K, T helper type 17 immune response plays an indispensable role for development of iodine-induced autoimmune thyroiditis in nonobese diabetic-H2h4 mice. Endocrinology 150, 5135–5142 (2009). [PubMed: 19797122]
16. Shi Y, Wang H, Su Z, Chen J, Xue Y, Wang S, Xue Y, He Z, Yang H, Zhou C, Kong F, Liu Y, Yang P, Lu L, Shao Q, Huang X, Xu H, Differentiation imbalance of Th1/Th17 in peripheral blood mononuclear cells might contribute to pathogenesis of Hashimoto's thyroiditis. Scand. J. Immunol 72, 250–255 (2010). [PubMed: 20696023]
17. Konca Degertekin C, Aktas Yilmaz B, Balos Toruner F, Kalkanci A, Turhan Iyidir O, Fidan I, Yesilyurt E, Cakir N, Kustimur S, Arslan M, Circulating Th17 cytokine levels are altered in Hashimoto's thyroiditis. Cytokine 80, 13–17 (2016). [PubMed: 26928603]
18. Rydzewska M, Jaromin M, Pasierowska IE, Stozek K, Bossowski A, Role of the T and B lymphocytes in pathogenesis of autoimmune thyroid diseases. Thyroid Res. 11, 1–11 (2018). [PubMed: 29375671]
19. Zhu C, Ma J, Liu Y, Tong J, Tian J, Chen J, Tang X, Xu H, Lu L, Wang S, Increased frequency of follicular helper T cells in patients with autoimmune thyroid disease. J. Clin. Endocrinol. Metab 97, 943–950 (2012). [PubMed: 22188745]
20. Kotwal A, Gustafson MP, Bornschlegl S, Kottschade L, Delivanis DA, Dietz AB, Gandhi M, Ryder M, Immune Checkpoint Inhibitor-Induced Thyroiditis Is Associated with Increased Intrathyroidal T Lymphocyte Subpopulations. Thyroid 30, 1440–1450 (2020). [PubMed: 32323619]
21. Angell TE, Min L, Wieczorek TJ, Hodi FS, Unique cytologic features of thyroiditis caused by immune checkpoint inhibitor therapy for malignant melanoma. Genes Dis. 5, 46–48 (2018). [PubMed: 29619406]
22. Lozano AX, Chaudhuri AA, Nene A, Bacchiocchi A, Earland N, Vesely MD, Usmani A, Turner BE, Steen CB, Luca BA, Badri T, Gulati GS, Vahid MR, Khameneh F, Harris PK, Chen DY, Dhodapkar K, Sznol M, Halaban R, Newman AM, T cell characteristics associated with toxicity to immune checkpoint blockade in patients with melanoma. Nat. Med 28, 353–362 (2022). [PubMed: 35027754]
23. von Euw E, Chodon T, Attar N, Jalil J, Koya RC, Comin-Anduix B, Ribas A, CTLA4 blockade increases Th17 cells in patients with metastatic melanoma. J. Transl. Med 7, 1–13 (2009). [PubMed: 19123955]
24. Herati RS, Knorr DA, Vella LA, Silva LV, Chilukuri L, Apostolidis SA, Huang AC, Muselman A, Manne S, Kuthuru O, Staupe RP, Adamski SA, Kannan S, Kurupati RK, Ertl HCJ, Wong JL, Bournazos S, McGettigan S, Schuchter LM, Kotecha RR, Funt SA, Voss MH, Motzer RJ, Lee C-H, Bajorin DF, Mitchell TC, V Ravetch J, Wherry EJ, PD-1 directed immunotherapy alters

Tfh and humoral immune responses to seasonal influenza vaccine. Nat. Immunol 23, 1183–1192 (2022). [PubMed: 35902637]

25. Nakamura Y, Biomarkers for Immune Checkpoint Inhibitor-Mediated Tumor Response and Adverse Events. Front. Med 6 (2019), doi:10.3389/fmed.2019.00119.
26. Axelrod ML, Meijers WC, Screever EM, Qin J, Carroll MG, Sun X, Tannous E, Zhang Y, Sugiura A, Taylor BC, Hanna A, Zhang S, Amancherla K, Tai W, Wright JJ, Wei SC, Opalenik SR, Toren AL, Rathmell JC, Ferrell PB, Phillips EJ, Mallal S, Johnson DB, Allison JP, Moslehi JJ, Balko JM, T cells specific for α-myosin drive immunotherapy-related myocarditis. Nature (2022), doi:10.1038/s41586-022-05432-3.
27. Sasson SC, Slevin SM, Cheung VTF, Nassiri I, Olsson-Brown A, Fryer E, Ferreira RC, Trzupek D, Gupta T, Al-Hillawi L, lenna Issaias M, Easton A, Campo L, FitzPatrick MEB, Adams J, Chitnis M, Protheroe A, Tuthill M, Coupe N, Simmons A, Payne M, Middleton MR, Travis SPL, Fairfax BP, Klenerman P, Brain O, Interferon-Gamma–Producing CD8+ Tissue Resident Memory T Cells Are a Targetable Hallmark of Immune Checkpoint Inhibitor–Colitis. Gastroenterology 161, 1229–1244.e9 (2021). [PubMed: 34147519]
28. Reschke R, Shapiro JW, Yu J, Rouhani SJ, Olson DJ, Zha Y, Gajewski TF, Checkpoint Blockade-Induced Dermatitis and Colitis Are Dominated by Tissue-Resident Memory T Cells and Th1/Tc1 Cytokines. Cancer Immunol. Res 10, 1167–1174 (2022). [PubMed: 35977003]
29. Luoma AM, Suo S, Williams HL, Sharova T, Sullivan K, Manos M, Bowling P, Hodi FS, Rahma O, Sullivan RJ, Boland GM, Nowak JA, Dougan SK, Dougan M, Yuan GC, Wucherpfennig KW, Molecular Pathways of Colon Inflammation Induced by Cancer Immunotherapy. Cell 182, 655–671.e22 (2020). [PubMed: 32603654]
30. Adam K, Iuga A, Tocheva AS, Mor A, A novel mouse model for checkpoint inhibitor-induced adverse events. PLoS One 16, 1–14 (2021).
31. Das S, Johnson DB, Immune-related adverse events and anti-tumor efficacy of immune checkpoint inhibitors. J. Immunother. Cancer 7, 1–11 (2019). [PubMed: 30612589]
32. Bocharnikov AV, Keegan J, Wacleche VS, Cao Y, Fonseka CY, Wang G, Muise ES, Zhang KX, Arazi A, Keras G, Li ZJ, Qu Y, Gurish MF, Petri M, Buyon JP, Putterman C, Wofsy D, James JA, Guthridge JM, Diamond B, Anolik JH, Mackey MF, Alves SE, Nigrovic PA, Costenbader KH, Brenner MB, Lederer JA, Rao DA, PD-1hiCXCR5- T peripheral helper cells promote B cell responses in lupus via MAF and IL-21. JCI Insight 4 (2019), doi:10.1172/jci.insight.130062.
33. Crotty S, Follicular helper CD4 T cells (TFH). Annu. Rev. Immunol 29, 621–663 (2011). [PubMed: 21314428]
34. Yoshitomi H, Ueno H, Shared and distinct roles of T peripheral helper and T follicular helper cells in human diseases. Cell. Mol. Immunol 18, 523–527 (2021). [PubMed: 32868910]
35. Rao DA, Gurish MF, Marshall JL, Slowikowski K, Fonseka CY, Liu Y, Donlin LT, Henderson LA, Wei K, Mizoguchi F, Teslovich NC, Weinblatt ME, Massarotti EM, Coblyn JS, Helfgott SM, Lee YC, Todd DJ, Bykerk VP, Goodman SM, Pernis AB, Ivashkiv LB, Karlson EW, Nigrovic PA, Filer A, Buckley CD, Lederer JA, Raychaudhuri S, Brenner MB, Pathologically expanded peripheral T helper cell subset drives B cells in rheumatoid arthritis. Nature 542, 110–114 (2017). [PubMed: 28150777]
36. Zander R, Kasmani MY, Chen Y, Topchyan P, Shen J, Zheng S, Burns R, Ingram J, Cui C, Joshi N, Craft J, Zajac A, Cui W, Tfh-cell-derived interleukin 21 sustains effector $CD8^+$ T cell responses during chronic viral infection. Immunity 55, 475–493.e5 (2022). [PubMed: 35216666]
37. Deng S, Sun Z, Qiao J, Liang Y, Liu L, Dong C, Shen A, Wang Y, Tang H, Fu YX, Peng H, Targeting tumors with IL-21 reshapes the tumor microenvironment by proliferating PD-1intTim-3-CD8+ T cells. JCI Insight 5 (2020), doi:10.1172/JCI.INSIGHT.132000.
38. Niogret J, Berger H, Rebe C, Mary R, Ballot E, Truntzer C, Thibaudin M, Derangère V, Hibos C, Hampe L, Rageot D, Accogli T, Joubert P, Routy B, Harker J, Vegran F, Ghiringhelli F, Chalmin F, Follicular helper-T cells restore CD8 + -dependent antitumor immunity and anti-PD-L1/PD-1 efficacy. J. Immunother. Cancer 9 (2021), doi:10.1136/jitc-2020-002157.
39. Annunziato F, Romagnani C, Romagnani S, The 3 major types of innate and adaptive cell-mediated effector immunity. J. Allergy Clin. Immunol 135, 626–635 (2015). [PubMed: 25528359]

40. Shi LZ, Fu T, Guan B, Chen J, Blando JM, Allison JP, Xiong L, Subudhi SK, Gao J, Sharma P, Interdependent IL-7 and IFN-γ signalling in T-cell controls tumour eradication by combined α-CTLA-4+α-PD-1 therapy. Nat. Commun 7 (2016), doi:10.1038/ncomms12335.

41. Gao J, Shi LZ, Zhao H, Chen J, Xiong L, He Q, Chen T, Roszik J, Bernatchez C, Woodman SE, Chen PL, Hwu P, Allison JP, Futreal A, Wargo JA, Sharma P, Loss of IFN-γ Pathway Genes in Tumor Cells as a Mechanism of Resistance to Anti-CTLA-4 Therapy. Cell 167, 397–404.e9 (2016). [PubMed: 27667683]

42. Kuriya G, Uchida T, Akazawa S, Kobayashi M, Nakamura K, Satoh T, Horie I, Kawasaki E, Yamasaki H, Yu L, Iwakura Y, Sasaki H, Nagayama Y, Kawakami A, Abiru N, Double deficiency in IL-17 and IFN-γ signalling significantly suppresses the development of diabetes in the NOD mouse. Diabetologia 56, 1773–1780 (2013). [PubMed: 23699989]

43. Kim CH, Greenberg HB, Butcher EC, Kim CH, Kunkel EJ, Boisvert J, Johnston B, Campbell JJ, Genovese MC, Greenberg HB, Butcher EC, Bonzo / CXCR6 expression defines type 1 – polarized T-cell subsets with extralymphoid tissue homing potential Find the latest version : Bonzo / CXCR6 expression defines type 1 – polarized T-cell subsets with extralymphoid tissue homing potential. 107, 595–601 (2001).

44. Gearty SV, Dündar F, Zumbo P, Espinosa-Carrasco G, Shakiba M, Sanchez-Rivera FJ, Socci ND, Trivedi P, Lowe SW, Lauer P, Mohibullah N, Viale A, DiLorenzo TP, Betel D, Schietinger A, An autoimmune stem-like CD8 T cell population drives type 1 diabetes. Nature 602, 156–161 (2022). [PubMed: 34847567]

45. Ciecko AE, Schauder DM, Foda B, Petrova G, Kasmani MY, Burns R, Lin C-W, Drobyski WR, Cui W, Chen Y-G, Self-Renewing Islet TCF1 + CD8 T Cells Undergo IL-27–Controlled Differentiation to Become TCF1 − Terminal Effectors during the Progression of Type 1 Diabetes . J. Immunol 207, 1990–2004 (2021). [PubMed: 34507949]

46. Dudek M, Pfister D, Donakonda S, Filpe P, Schneider A, Laschinger M, Hartmann D, Hüser N, Meiser P, Bayerl F, Inverso D, Wigger J, Sebode M, Öllinger R, Rad R, Hegenbarth S, Anton M, Guillot A, Bowman A, Heide D, Müller F, Ramadori P, Leone V, Garcia-Caceres C, Gruber T, Seifert G, Kabat AM, Malm JP, Reider S, Effenberger M, Roth S, Billeter AT, Müller-Stich B, Pearce EJ, Koch-Nolte F, Käser R, Tilg H, Thimme R, Böttler T, Tacke F, Dufour JF, Haller D, Murray PJ, Heeren R, Zehn D, Böttcher JP, Heikenwälder M, Knolle PA, Auto-aggressive CXCR6+ CD8 T cells cause liver immune pathology in NASH (2021).

47. Leonard WJ, Wan CK, IL-21 Signaling in Immunity. F1000Research 5, 1–10 (2016).

48. Álvarez-Sierra D, Marín-Sánchez A, Ruiz-Blázquez P, de Jesús Gil C, Iglesias-Felip C, González Ó, Casteras A, Costa RF, Nuciforo P, Colobran R, Pujol-Borrell R, Analysis of the PD-1/PD-L1 axis in human autoimmune thyroid disease: Insights into pathogenesis and clues to immunotherapy associated thyroid autoimmunity. J. Autoimmun 103 (2019), doi:10.1016/j.jaut.2019.05.013.

49. Bluestone JA, Anderson M, Herold KC, Stamatouli AM, Quandt Z, Perdigoto AL, Clark PL, Kluger H, Weiss SA, Gettinger S, Sznol M, Young A, Rushakoff R, Lee J, in Diabetes, (American Diabetes Association Inc., 2018), vol. 67, pp. 1471–1480. [PubMed: 29937434]

50. Lowery FJ, Krishna S, Yossef R, Parikh NB, Chatani PD, Zacharakis N, Parkhurst MR, Levin N, Sindiri S, Sachs A, Hitscherich KJ, Yu Z, Vale NR, Lu YC, Zheng Z, Jia L, Gartner JJ, Hill VK, Copeland AR, Nah SK, Masi RV, Gasmi B, Kivitz S, Paria BC, Florentin M, Kim SP, Hanada KI, Li YF, Ngo LT, Ray S, Shindorf ML, Levi ST, Shepherd R, Toy C, Parikh AY, Prickett TD, Kelly MC, Beyer R, Goff SL, Yang JC, Robbins PF, Rosenberg SA, Molecular signatures of antitumor neoantigen-reactive T cells from metastatic human cancers. Science (80-.). 375, 877–884 (2022).

51. Yost KE, Satpathy AT, Wells DK, Qi Y, Kageyama R, Mcnamara K, Granja JM, Sarin KY, Brown RA, Gupta RK, Curtis C, Bucktrout SL, Clonal replacement of tumor-specific T cells following PD-1 blockade. 25, 1251–1259 (2020).

52. Oh DY, Kwek SS, Raju SS, Li T, McCarthy E, Chow E, Aran D, Ilano A, Pai CCS, Rancan C, Allaire K, Burra A, Sun Y, Spitzer MH, Mangul S, Porten S, Meng MV, Friedlander TW, Ye CJ, Fong L, Intratumoral CD4+ T Cells Mediate Anti-tumor Cytotoxicity in Human Bladder Cancer. Cell 181, 1612–1625.e13 (2020). [PubMed: 32497499]

53. Thommen DS, Koelzer VH, Herzig P, Roller A, Trefny M, Dimeloe S, Kiialainen A, Hanhart J, Schill C, Hess C, Prince SS, Wiese M, Lardinois D, Ho PC, Klein C, Karanikas V, Mertz KD, Schumacher TN, Zippelius A, A transcriptionally and functionally distinct pd-1+ cd8+ t cell pool

with predictive potential in non-small-cell lung cancer treated with pd-1 blockade. Nat. Med 24, 994–1004 (2018). [PubMed: 29892065]

54. Kotwal A, Kottschade L, Ryder M, PD-L1 Inhibitor-Induced Thyroiditis Is Associated with Better Overall Survival in Cancer Patients. Thyroid 30, 1–8 (2020). [PubMed: 31842720]
55. Cheung Y-MM, Wang W, McGregor B, Hamnvik O-PR, Associations between immune-related thyroid dysfunction and efficacy of immune checkpoint inhibitors: a systematic review and meta-analysis. Cancer Immunol. Immunother 71, 1795–1812 (2022). [PubMed: 35022907]
56. Muir CA, Clifton-Bligh RJ, V Long G, Scolyer RA, Lo SN, Carlino MS, Tsang VHM, Menzies AM, Thyroid immune-related adverse events following immune checkpoint inhibitor treatment. J. Clin. Endocrinol. Metab (2021), doi:10.1210/clinem/dgab263.
57. Shankar B, Zhang J, Naqash AR, Forde PM, Feliciano JL, Marrone KA, Ettinger DS, Hann CL, Brahmer JR, Ricciuti B, Owen D, Toi Y, Walker P, Otterson GA, Patel SH, Sugawara S, Naidoo J, Multisystem Immune-Related Adverse Events Associated with Immune Checkpoint Inhibitors for Treatment of Non-Small Cell Lung Cancer. JAMA Oncol. 6, 1952–1956 (2020). [PubMed: 33119034]
58. Hata H, Matsumura C, Chisaki Y, Nishioka K, Tokuda M, Miyagi K, Suizu T, Yano Y, A Retrospective Cohort Study of Multiple Immune-Related Adverse Events and Clinical Outcomes Among Patients With Cancer Receiving Immune Checkpoint Inhibitors. Cancer Control 29, 1–12 (2022).
59. Scott ES, Long GV, Guminski A, Clifton-Bligh RJ, Menzies AM, Tsang VH, The spectrum, incidence, kinetics and management of endocrinopathies with immune checkpoint inhibitors for metastatic melanoma. Eur. J. Endocrinol 178, 173–180 (2018). [PubMed: 29187509]
60. Kotwal A, Haddox C, Block M, Kudva YC, Immune checkpoint inhibitors: An emerging cause of insulin-dependent diabetes. BMJ Open Diabetes Res. Care 7 (2019), doi:10.1136/bmjdrc-2018-000591.
61. Ueda H, Howson JMM, Esposito L, Heward J, Snook H, Chamberlain G, Rainbow DB, Hunter KMD, Smith AN, Di Genova G, Herr MH, Dahlman I, Payne F, Smyth D, Lowe C, Twells RCJ, Howlett S, Healy B, Nutland S, Rance HE, Everett V, Smink LJ, Lam AC, Cordell HJ, Walker NM, Bordin C, Hulme J, Motzo C, Cucca F, Hess JF, Metzker ML, Rogers J, Gregory S, Allahabadia A, Nithiyananthan R, Tuomilehto-Wolf E, Tuomilehto J, Bingley P, Gillespie KM, Undlien DE, Rønningen KS, Guja C, Ionescu-Tirgovişte C, Savage DA, Maxwell AP, Carson DJ, Patterson CC, Franklyn JA, Clayton DG, Peterson LB, Wicker LS, Todd JA, Gough SCL, Association of the T-cell regulatory gene CTLA4 with susceptibility to autoimmune disease. Nature 423, 506–511 (2003). [PubMed: 12724780]
62. Hasan Ali O, Berner F, Bomze D, Fässler M, Diem S, Cozzio A, Jörger M, Früh M, Driessen C, Lenz TL, Flatz L, Human leukocyte antigen variation is associated with adverse events of checkpoint inhibitors. Eur. J. Cancer 107, 8–14 (2019). [PubMed: 30529903]
63. Yano S, Ashida K, Sakamoto R, Sakaguchi C, Ogata M, Maruyama K, Sakamoto S, Ikeda M, Ohe K, Akasu S, Iwata S, Wada N, Matsuda Y, Nakanishi Y, Nomura M, Ogawa Y, Human leucocyte antigen DR15, a possible predictive marker for immune checkpoint inhibitor–induced secondary adrenal insufficiency. Eur. J. Cancer 130, 198–203 (2020). [PubMed: 32229416]
64. Khan Z, Di Nucci F, Kwan A, Hammer C, Mariathasan S, Rouilly V, Carroll J, Fontes M, Acosta SL, Guardino E, Chen-Harris H, Bhangale T, Mellman I, Rosenberg J, Powles T, Hunkapiller J, Chandler GS, Albert ML, Polygenic risk for skin autoimmunity impacts immune checkpoint blockade in bladder cancer. Proc. Natl. Acad. Sci. U. S. A 117, 12288–12294 (2020). [PubMed: 32430334]
65. Quandt A, Kim S, Villanueva-Meyer J, Coupe C, Young A, Kang J, Schmajuk G, Rush S, Ziv E, Perdigoto A, Herold K, Lechner M, Su M, Tyrrell J, Bluestone J, Anderson M, Masharani U, Spectrum of Clinical Presentations, Imaging Findings and HLA types in Immune Checkpoint Inhibitor Induced Hypophysitis. J. Endocr. Soc , In press (2023).
66. Anderson MS, Bluestone JA, THE NOD MOUSE: A Model of Immune Dysregulation. Annu. Rev. Immunol 23, 447–485 (2005). [PubMed: 15771578]
67. Zhou Y, Zhou B, Pache L, Chang M, Khodabakhshi AH, Tanaseichuk O, Benner C, Chanda SK, Metascape provides a biologist-oriented resource for the analysis of systems-level datasets. Nat. Commun 10 (2019), doi:10.1038/s41467-019-09234-6.

68. Zhang L, Yu X, Zheng L, Zhang Y, Li Y, Fang Q, Gao R, Kang B, Zhang Q, Huang JY, Konno H, Guo X, Ye Y, Gao S, Wang S, Hu X, Ren X, Shen Z, Ouyang W, Zhang Z, Lineage tracking reveals dynamic relationships of T cells in colorectal cancer. Nature 564, 268–272 (2018). [PubMed: 30479382]

69. Stuart T, Butler A, Hoffman P, Hafemeister C, Papalexi E, Mauck WM, Hao Y, Stoeckius M, Smibert P, Satija R, Comprehensive Integration of Single-Cell Data. Cell 177, 1888–1902.e21 (2019). [PubMed: 31178118]

70. Tirosh I, Izar B, Prakadan SM, Wadsworth MH, Treacy D, Trombetta JJ, Rotem A, Rodman C, Lian C, Murphy G, Fallahi-Sichani M, Dutton-Regester K, Lin JR, Cohen O, Shah P, Lu D, Genshaft AS, Hughes TK, Ziegler CGK, Kazer SW, Gaillard A, Kolb KE, Villani AC, Johannessen CM, Andreev AY, Van Allen EM, Bertagnolli M, Sorger PK, Sullivan RJ, Flaherty KT, Frederick DT, Jané-Valbuena J, Yoon CH, Rozenblatt-Rosen O, Shalek AK, Regev A, Garraway LA, Dissecting the multicellular ecosystem of metastatic melanoma by single-cell RNA-seq. Science (80-.). 352, 189–196 (2016).

71. Chen EY, Tan CM, Kou Y, Duan Q, Wang Z, Meirelles GV, Clark NR, Ma'ayan A, Enrichr: interactive and collaborative HTML5 gene list enrichment analysis tool. BMC Bioinformatics 14, 128 (2013). [PubMed: 23586463]

72. Heng TSP, Painter MW, The Immunological Genome Project: networks of gene expression in immune cells. Nat. Immunol 9, 1091–1094 (2008). [PubMed: 18800157]

73. 9 Street Kelly1,8,DavideRisso2, Fletcher Russell B.3,DiyaDas3,9, Ngai John3,6,7,Yosef Nir4,8, Purdom Elizabeth5,8 and Dudoit Sandrine1,5,8, Slingshot: cell lineage and pseudotime inference for single-cell transcriptomics. , 1–16 (2010).

74. Borcherding N, Bormann NL, Kraus G, scRepertoire: An R-based toolkit for single-cell immune receptor analysis. F1000Research 9, 1–17 (2020).

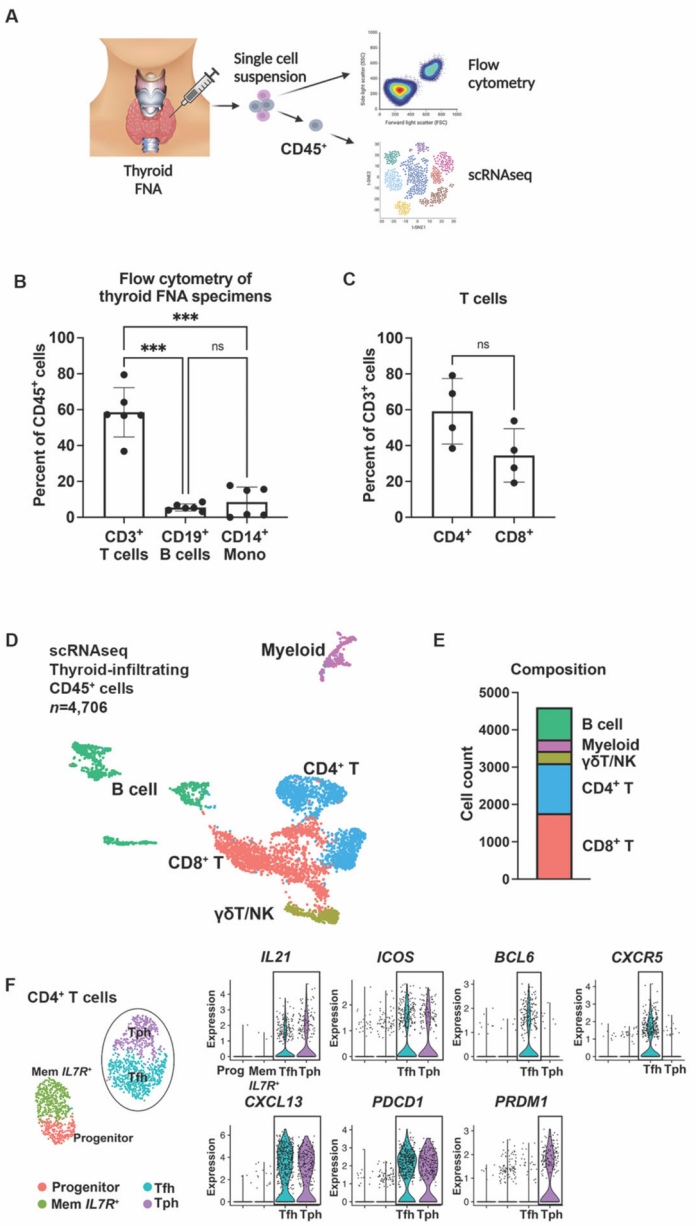

Fig. 1. Thyroid-infiltrating immune populations in ICI-thyroiditis patients are T cell-predominant and include IL-21$^+$ CD4$^+$ Tfh and Tph cells.

(A) Shown is a schema of thyroid specimen collection by FNA. **(B)** Immune populations were analyzed by flow cytometry in thyroid FNA specimens (n=6 patients). Mono, monocytes. Data were analyzed with an ANOVA with Welch's correction. **(C)** T cell populations were analyzed by flow cytometry in thyroid FNA specimens (n=4 patients). Data were analyzed with a t test with Welch's correction. In (B and C), data are presented as mean±SD. **(D)** Shown is a UMAP representing scRNAseq analysis of thyroid infiltrating CD45$^+$ immune cells (n=5 patients). **(E)** Shown is the distribution of intrathyroidal cells by major immune population. **(F)** UMAP of subclustered CD4$^+$ T cells (left) and violin plots show genes associated with T follicular (Tfh) and peripheral (Tph) helper populations (right). ***p<0.001; ns, not significant.

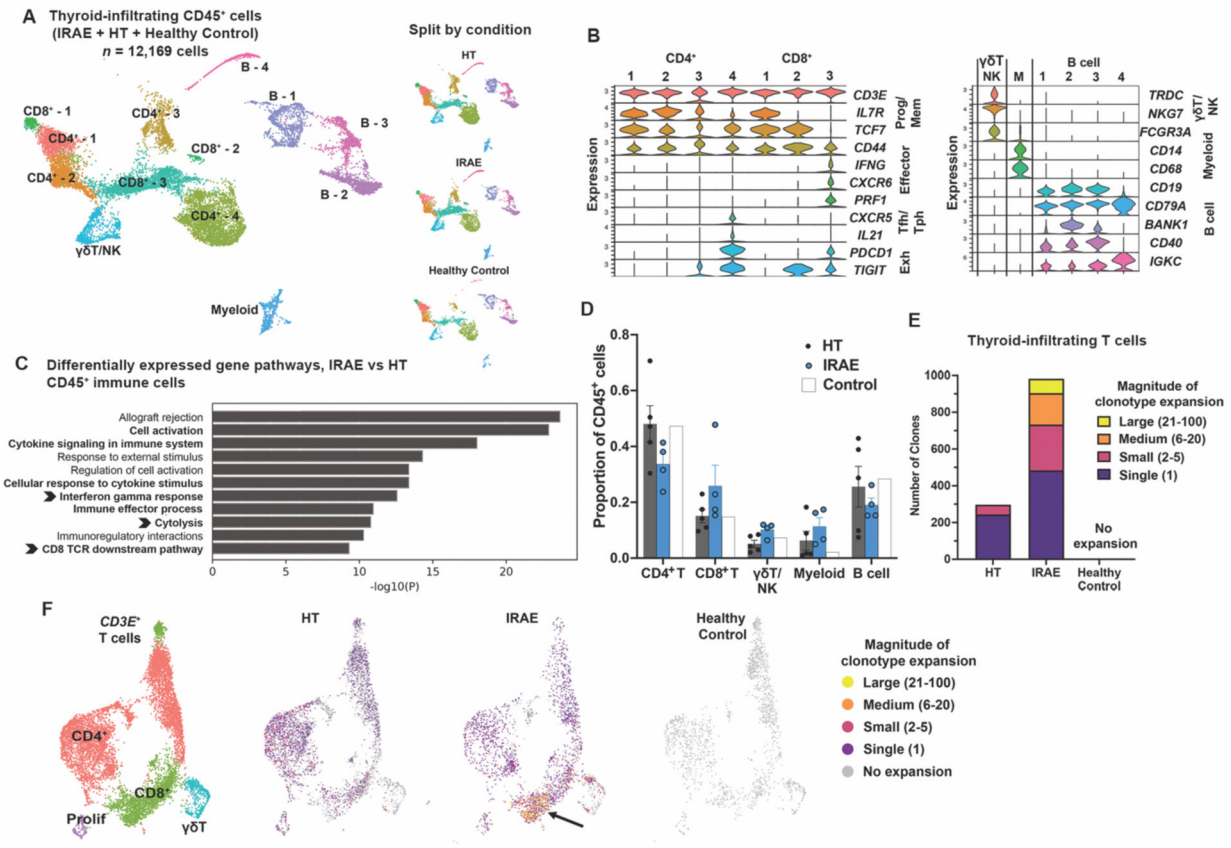

Fig. 2. CD8$^+$ T cells are expanded in ICI-thyroiditis compared to HT.

(A) Thyroid immune infiltrates were compared in samples from individuals with ICI-thyroiditis (IRAE, *n*=5), Hashimoto's thyroiditis (HT, *n*=5) and healthy controls (*n*=3, pooled) by scRNAseq. Shown is a UMAP of integrated CD45$^+$ cells across conditions (left), with UMAP plots split by condition on the right. **(B)** Gene expression across immune cell clusters in ICI-thyroiditis is shown. Stacked violin plot show gene expression by cell cluster for CD4$^+$ and CD8$^+$ T cells (left) and other immune cell populations (right), including γδ T, NK, myeloid (M), and B cell populations. **(C)** Shown is pathway analysis of differentially expressed genes in thyroid-infiltrating CD45$^+$ cells between IRAE and HT. Bolded pathways indicate those associated with immune activation. Arrowheads indicate pathways related to effector CD8$^+$ T cell functions. **(D)** Shown is the distribution of intrathyroidal cells by major immune population by condition, presented as mean±SEM. Data were analyzed by ANOVA; p=ns **(E)** The frequency of clonotype expansion of intrathyroidal CD3$^+$ T cells is shown by thyroid state. **(F)** Shown are UMAPs of thyroid-infiltrating CD3$^+$ cells (left) and clonotype distribution split by thyroid condition (right). The arrow indicates a cluster with medium to large clonal expansion.

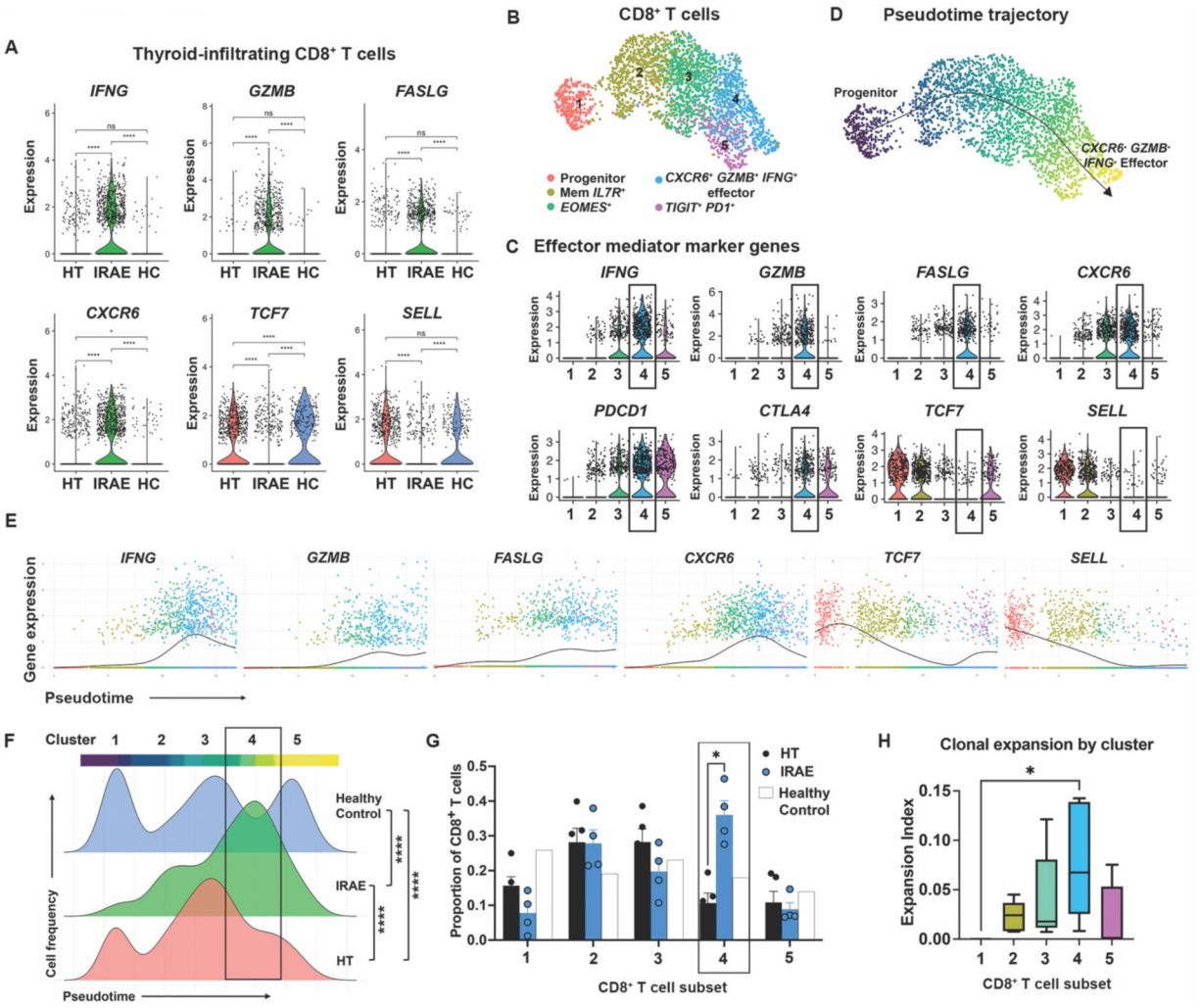

Fig. 3. Clonally expanded *CXCR6*$^+$ *IFNG*$^+$ *GZMB*$^+$ effector CD8$^+$ T cells distinguish ICI-thyroiditis.

(A) CD8$^+$ T cell gene expression is shown by thyroid state (HT, n=5; IRAE, n=5; and HC, n=3, pooled). **(B)** Shown is a UMAP of subclustered thyroid-infiltrating CD8$^+$ T cells. Mem, memory. **(C)** Gene expression is shown across the CD8$^+$ subclusters. **(D)** Slingshot trajectory analysis of CD8$^+$ T cell populations is shown. Effector population Cluster 4 is boxed. **(E)** Transcriptional transitions in CD8$^+$ T cells are shown along the pseudotime trajectory. **(F)** Density distribution of CD8$^+$ T cell along the pseudotime trajectory are shown split by thyroid state. **(G)** Shown is a comparison of the subset frequency between IRAE and HT; pooled HC specimens are also shown. Data are presented as mean±SEM. **(H)** STARTRAC clonal expansion index is shown by CD8$^+$ subcluster. The box and whisker plots indicate median, 1.5 times the interquartile range, minimum, and maximum values. Data were analyzed with ANOVA with Welch correction (A), asymptotic Kolmogorov-Smirnov test (F), Student's t test with correction for multiple comparisons (G), or ANOVA with Tukey's multiple comparison's test (H); *p<0.05, ***p<0.001, ****p<0.0001.

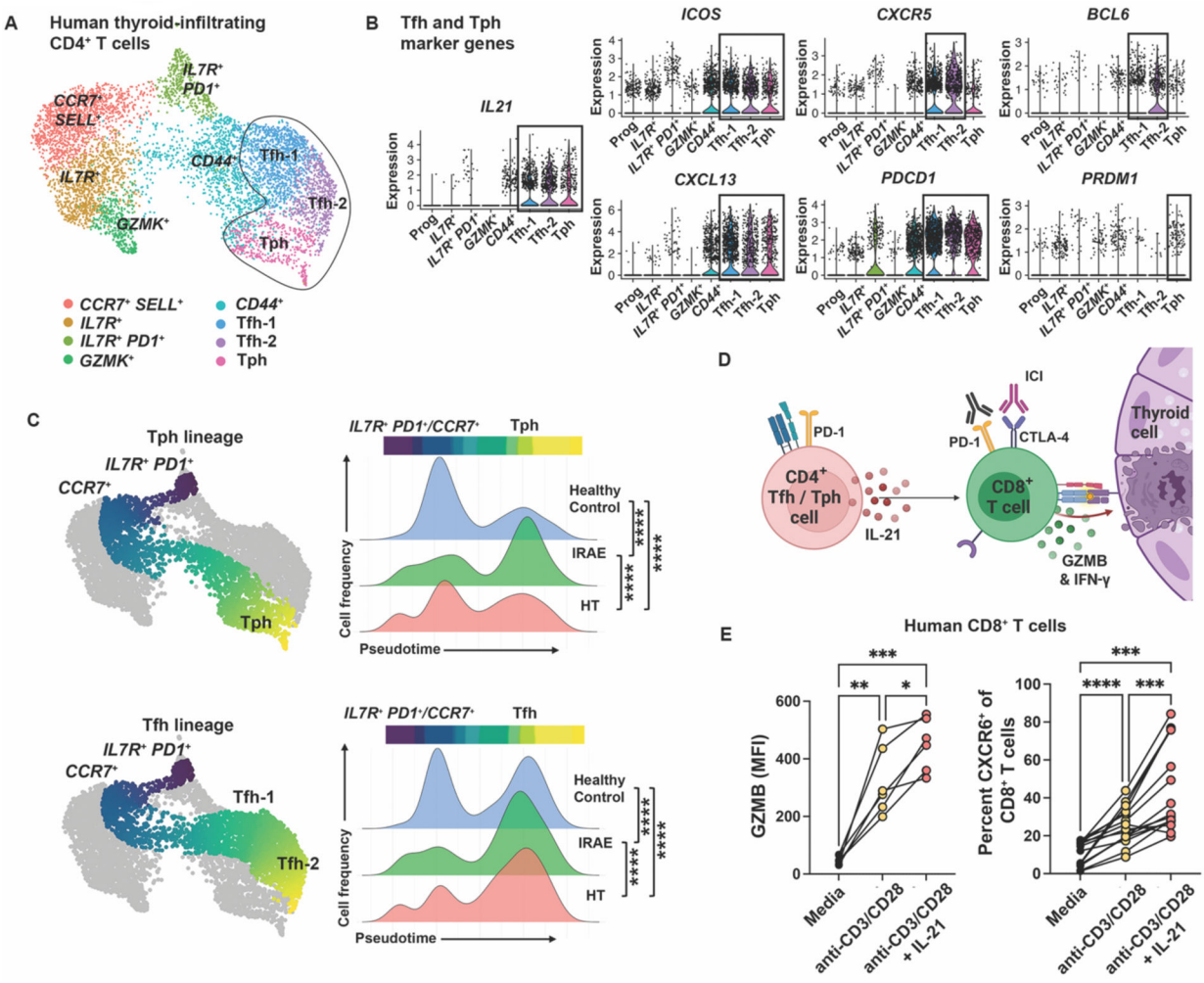

Fig. 4. IL-21$^+$ CD4$^+$ T follicular helper (Tfh) and peripheral helper (Tph) cells are enriched in ICI-thyroiditis and promote CD8$^+$ T cell thyrotoxicity.

(A) Shown is a UMAP of subclustered thyroid infiltrating CD4$^+$ T cells in human FNA specimens by scRNAseq (HT, n=5; IRAE, n=5; and HC, n=3, pooled). **(B)** Expression of Tfh and Tph marker genes are shown by cluster. **(C)** Trajectory analysis of CD4$^+$ T cells by Slingshot and density distribution along the pseudotime trajectory are shown by condition for two lineages: Tph (left) and Tfh (right). **(D)** Proposed action of Tfh and Tph cells on effector CD8$^+$ T cells in ICI-thyroiditis. **(E)** Granzyme B (GZMB) expression on human CD8$^+$ T cells (median fluorescence intensity, MFI) and the frequency of CXCR6$^+$ cells of CD8$^+$ T cells were quantified following in vitro stimulation with anti-CD3/CD28 beads and recombinant human IL-21; samples evaluated after 3 days by flow cytometry. Each set of linked points represents data from one participant; data shown from two experiments. Data were analyzed with asymptotic Kolmogorov-Smirnov test (C) or repeated measure ANOVA and subsequent Tukey's multiple pairwise comparisons (E). *p<0.05, **p<0.01, ***p<0.001, ****p<0.0001.

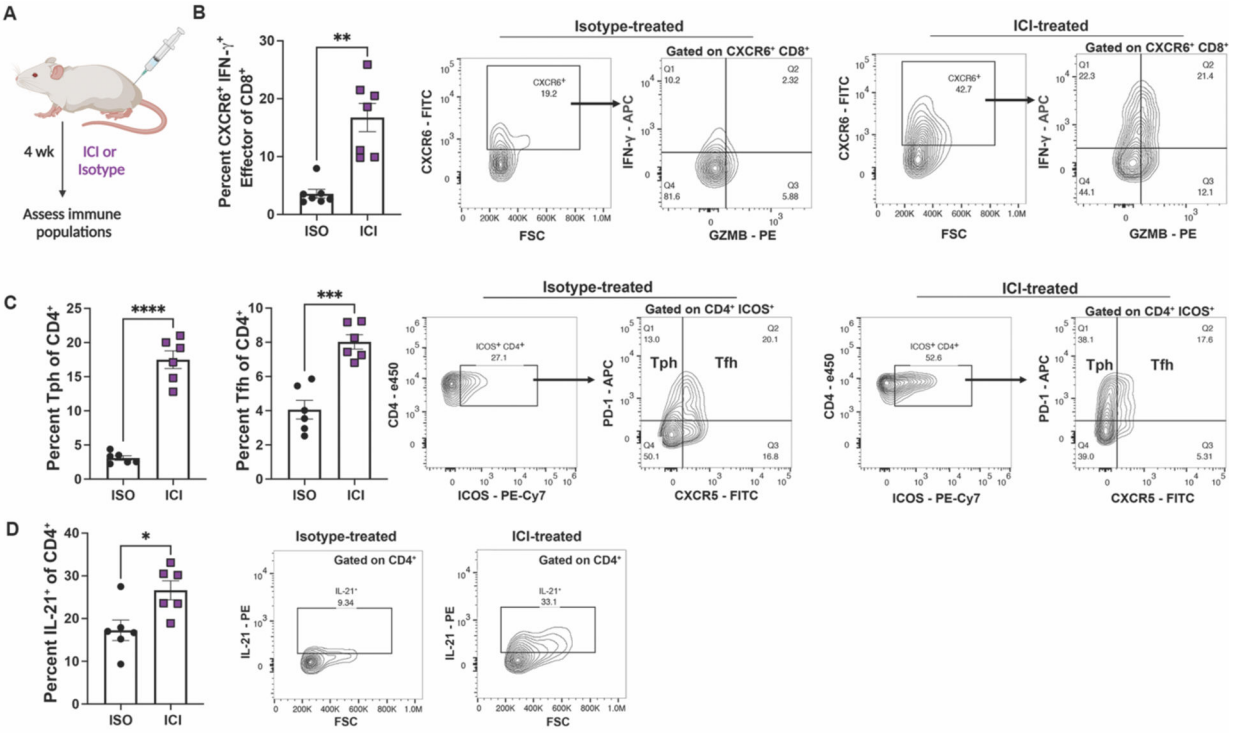

Fig. 5. CD8$^+$ effector T cells and IL-21$^+$ Tfh and Tph cells are increased in a mouse model of ICI-associated autoimmunity.

(A) Schematic of mouse model, where non-obese diabetic (NOD) mice are treated with anti-PD-1 + anti-CTLA-4 (ICI) or isotype control (ISO) for four weeks (wk) (n=6–7 per group). **(B)** Shown is the frequency of effector mediator CD8$^+$ T cells in spleen of ICI treated mice; representative flow plots are shown on the right. FSC, forward scatter; FITC, fluorescein isothiocyanate; PE, phycoerythrin; APC, allophycocyanin. **(C)** Shown are the frequencies and representative flow plots of T peripheral (Tph: CD4$^+$ PD-1$^+$ ICOS$^+$ CXCR5$^-$) and T follicular (Tfh: CD4$^+$ PD-1$^+$ ICOS$^+$ CXCR5$^+$) helper cells in spleen. **(D)** Shown is the frequency of IL-21$^+$ CD4$^+$ T cells in spleen; representative flow plots are shown on the right. Each point represents data from one animal (B to D), and representative data shown from one of two independent experiments. Data are presented as mean±SEM and were analyzed by unpaired Student's t test with Welch correction (B to D); *p<0.05, **p<0.01, ***p<0.001, ****p<0.0001.

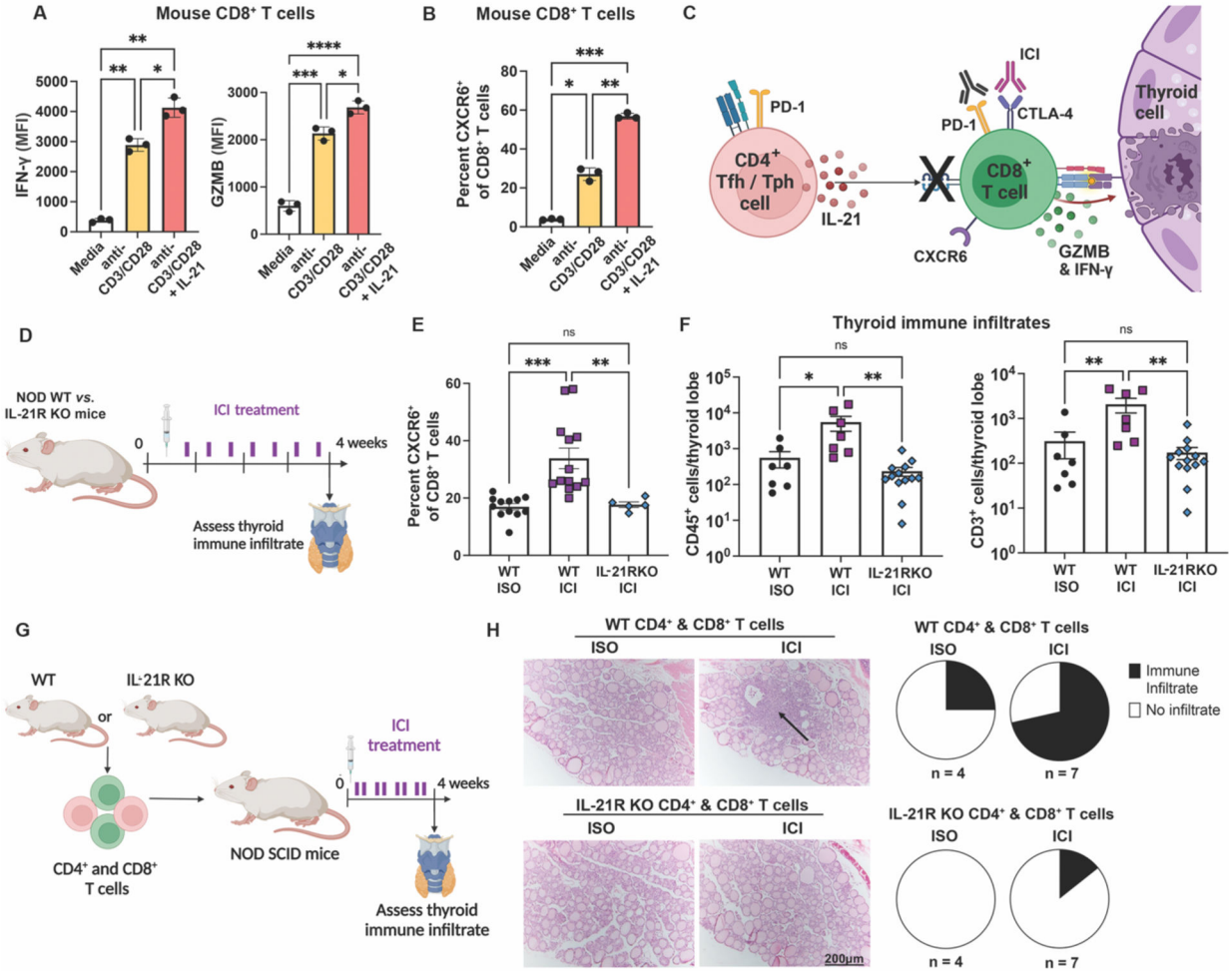

Fig. 6. IL-21 signaling is required for ICI-related thyroid autoimmunity in a mouse model.

(A and B) Shown is expression of effector molecules IFN-γ and GZMB by $CD8^+$ T cells **(A)** and the frequency of $CXCR6^+$ cells of murine $CD8^+$ T cells **(B)** stimulated 3 days in vitro with anti-CD3/CD28 and recombinant murine IL-21, and then analyzed by flow cytometry (*n*=3 per group). Data from one representative experiment shown. **(C)** Proposed mechanism of ICI-thyroiditis and inhibition by deletion of IL-21 signaling. **(D)** Shown is a schematic of anti-PD-1 + anti-CTLA-4 (ICI) treatment in NOD wild type (WT) or IL-21R KO mice. **(E)** Shown is the frequency of $CXCR6^+$ $CD8^+$ T cells of total $CD8^+$ T cells in ICI (*n*=13) or isotype (ISO)-treated WT (*n*=12) and IL-21R KO mice spleens (*n*=5). **(F)** Thyroid-infiltrating $CD45^+$ and $CD3^+$ cells were quantified in ICI (*n*=7) or ISO-treated WT (*n*=7) and ICI-treated IL-21R KO mice (*n*=13). Each dot represents data from one animal, and data are pooled from three experiments. Data are presented as mean±SD (A,B) or mean±SEM (E,F) and were analyzed with ANOVA with Welch's correction and subsequent Tukey's pairwise comparison (A, B, E, and F), *p<0.05, **p<0.01, ***p<0.001, ****p<0.0001. **(G)** Shown is a schematic of ICI treatment of NOD.SCID mice after adoptive transfer of $CD4^+$ and $CD8^+$ T cells from WT or IL-21R KO mice. **(H)** Shown are representative thyroid histology sections of ICI or ISO-treated reconstituted NOD.SCID mice (left; H&E staining, original magnification 100x) and

cumulative incidence of thyroiditis by histology (right; black = immune infiltrate, white = no infiltrate). The arrow indicates area of immune infiltrate.